

UCSF

UC San Francisco Electronic Theses and Dissertations

Title

LC3-dependent EV loading and secretion (LDELS) promotes transferrin receptor secretion via extracellular vesicles

Permalink

<https://escholarship.org/uc/item/8k03z03m>

Author

Gardner, Jackson

Publication Date

2022

Peer reviewed|Thesis/dissertation

LC3-dependent EV loading and secretion (LDELS) promotes transferrin receptor secretion via extracellular vesicles

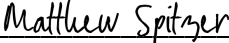
by
Jackson Gardner

DISSERTATION
Submitted in partial satisfaction of the requirements for degree of
DOCTOR OF PHILOSOPHY

in
Biomedical Sciences

in the
GRADUATE DIVISION
of the
UNIVERSITY OF CALIFORNIA, SAN FRANCISCO

Approved:


DocuSigned by:

4793AE6232BE479... Matthew Spitzer
Chair

DocuSigned by:

4F0... Jayanta Debnath

DocuSigned by:

4F0... K. Mark Ansel

DocuSigned by:

074A44F86EC2405... Melissa Reeves

Committee Members

Acknowledgements

Here I would like to thank the people who supported me with the kindness, guidance, and encouragement that allowed me to complete my doctoral degree. Firstly, I would like to thank my thesis advisor, Jay Debnath, who has provided constant support for my career goals since the day I joined his lab. Moving from science to consulting is not a very intuitive change, but Jay always supported my changing goals throughout the process. Jay is always able to keep a rational, level-headed perspective that makes the ups and downs of science significantly more bearable. At times when negative results were sending me spiraling, Jay was fantastic at calming my worries, highlighting the silver linings, and reorienting me in the right direction. I have learned a great deal from Jay about asking the right questions, identifying the tools to explore those questions, and compiling the results, both expected and unexpected, into appropriate answers. I'm sure these skills will assist me in my future career. Thank you, Jay!

I am also extremely thankful for the esteemed scientists who served on my thesis committee: Matthew Spitzer, Melissa Reeves, and Mark Ansel. Thank you for the constant support, accessibility, and interesting questions. I specifically chose each of you not only for your scientific expertise, but also because you have made me feel incredibly supported as a human being. Your insights into building a complete story and finding the right questions were essential in pushing my project through to completion. Additionally, I want to thank you for the career and professional advice over the years that allowed me to obtain my dream job!

During my graduate studies, several amazing individuals have made my research pursuits possible and productive. I would like to thank all the past and current members of the Debnath lab for their critical insights and contributions, both technically and intellectually. Specifically, I would like to thank Andrew Leidal for training me in nearly all of the experimental techniques and

foundational knowledge required to successfully navigate my research project. Thank you for constantly providing advice and support all along the way. Thanks to Tan Nguyen for endless technical support and for being so accessible and comforting whenever I was having a hard time. Thank you both for the many laughs. Thanks to Teresa Monkkonen, Gourish Mondal, Ariadne Vlahakis, and Sofia Bustamante Eguiguren for supporting me, for the good times, and for keeping the lab in working order. Lastly, I want to thank the UCSF BMS administration, especially Demian Sainz, for providing career support and excellent advice about navigating life as a graduate student in San Francisco.

My pursuit of a doctoral degree would not have been possible without my previous lab members from the Sonnenburg Lab at Stanford University, whom I got to know when I worked there as a laboratory technician. I am endlessly grateful for the guidance and mentorship of Justin and Erica Sonnenburg and Andrew Hryckowian. Thank you for cultivating my passion for biology and preparing me for my graduate studies. Thanks to all of my Bay Area friends from my time as an undergraduate at UC Davis and to the amazing new friends I made in graduate school. We have had many incredible adventures that truly made this time possible and enjoyable. Finally, I want to thank my parents, Christopher and Melissa, and my amazing siblings, Colin, Joshua, Zachary, and Alicia. I am the person I am today because of your love and support! And of course, I want to thank my dog Waldo for being the best dog in the world and getting me through all times, good and bad, for the last eight wonderful years.

Content in the following chapter was modified from the following publication:

Gardner JO, Leidal AM, Nguyen TA, Debnath J. LC3-dependent EV loading and secretion (LDELS) promotes TFRC (transferrin receptor) secretion via extracellular vesicles. *Autophagy*. 2022. PMID: 36286616.

Contributions: I was primarily responsible for writing the content in the first draft of this manuscript and Jay Debnath supervised this project. Together we edited and revised subsequent drafts.

**LC3-dependent EV loading and secretion (LDELS) promotes transferrin receptor
secretion via extracellular vesicles**

Jackson Oliveira Gardner

Abstract

Autophagy is traditionally described as an autodigestive pathway in which cells perform the orderly degradation and recycling of dysfunctional or unneeded cytosolic components within autophagosomes. However, autophagy also has its less intuitive but biologically distinct roles in secretion. These secretory functions, collectively termed secretory autophagy, range from the secretion of inflammatory cytokines to the biogenesis of extracellular vesicles (EVs). The study of EVs has generated significant interest of late given their ability to evoke intercellular communication and non-cell autonomous activity in both normal homeostatic cell activity and pathological settings. However, these exciting phenotypic applications have somewhat overtaken the spotlight of EV research leading investigations of the specific molecular components involved in EV loading and secretion to fall by the wayside. Further research is needed detailing the underlying mechanistic components of EV secretion if we are to fully understand and take advantage of the exciting capabilities of EVs in health and disease.

Recently, our lab described a secretory autophagy pathway termed LC3-dependent EV loading and secretion (LDELS) that facilitates the packaging of cytosolic cargoes, particularly RNA-binding proteins (RBPs), into extracellular vesicles for secretion outside the cell. The LDELS pathway utilizes a pool of LC3, a member of the ATG8 protein family that functions in autophagy substrate selection, localized at single membrane endosomes rather than double membrane autophagosomes. While our previous study focused on the requirement for this pathway

in the secretion of soluble RNA-binding proteins, we also observed a collection of proteins containing membrane-spanning regions that relied on this pathway for secretion. In particular, we identified transferrin receptor as a novel substrate of the LDELS pathway. Transferrin receptor is a membrane glycoprotein responsible for cellular iron uptake and has been implicated in diseases such as hematological disorders, neurodegenerative diseases, and cancer. Additionally, it was the first protein identified to be secreted in EVs.

Similar to other LDELS targets, TFRC secretion via EVs genetically requires components of the LC3-conjugation machinery but is independent of other *ATGs* involved in classical autophagosome formation. Interestingly, the secretion of EV-associated TFRC is actually enhanced upon inhibition of classical degradative capabilities. Furthermore, TFRC binds ATG8 orthologs via a cytoplasmic domain LC3-interacting region (LIR) motif, which may facilitate the loading of TFRC into EVs. However, this LIR motif is not solely responsible for the functional secretion of TFRC. This may be explained by the observation that TFRC exists both in the conventionally annotated orientation *and* in a reversed orientation in EVs, thus LC3 residing within the lumen of EVs may interact with LIRs localized to either the cytoplasmic *or* extracellular domains of TFRC. Additionally, the packaging and secretion of TFRC into EVs depends on multiple ESCRT pathway components, suggesting the ESCRT pathway is involved in the budding of TFRC into intraluminal vesicles, the precursors of EVs. Lastly, the secretion of TFRC requires the RAB27A, a small GTPase implicated in the docking and release of EVs into the extracellular space. Based on these results, we propose that the LDELS pathway promotes the TFRC incorporation into EVs and its secretion outside the cell.

Table of Contents

Chapter 1: Introduction	1
Autophagy	2
Overview of Secretory Autophagy	3
Extracellular Vesicles	3
Transferrin Receptor	4
Autophagy in Extracellular Vesicles Biogenesis.....	5
Chapter 2: LC3-dependent EV loading and secretion (LDELS) promotes transferrin receptor secretion via extracellular vesicles	7
Summary.....	8
Introduction	9
Results	11
Discussion.....	16
Experimental Procedures	29
Chapter 3: Summary Discussion and Future Perspectives.....	37
References	45

List of Figures

Chapter 2: LC3-dependent EV loading and secretion (LDELS) promotes transferrin receptor secretion via extracellular vesicles.....	7
Figure 2.1: ATG7 is genetically required for the secretion of transmembrane proteins via extracellular vesicles.....	19
Figure 2.2: Transferrin receptor (TFRC) secretion in EVs requires the LC3-conjugation pathway but is independent of other components mediating classical autophagosome formation.....	21
Figure 2.3: ATG8 family proteins bind TFRC via a cytoplasmic domain LIR motif.....	22
Figure 2.4: ESCRT machinery and RAB27A promotes TFRC loading and secretion via EVs. ...	25
Supplementary Figure 2.1: ATG12 is genetically required for the secretion of transmembrane proteins via extracellular vesicles.....	26
Supplementary Figure 2.2: Deletion of the TFRC cytoplasmic domain or mutation of the cytoplasmic domain LIR is not sufficient to disrupt TFRC co-immunoprecipitation with ATG8 family proteins.....	27
Chapter 3: Summary Discussion and Future Perspectives.....	37
Supplemental Figure 3.1: Proposed model for TFRC secretion in EVs via the LC3-dependent EV loading and secretion (LDELS) pathway.	44

List of Tables

Supplementary Table 2.1: Proteins identified from quantitative proteomic datasets of EVP fractions collected from control (WT) vs. <i>ATG7</i> ^{-/-} or <i>ATG12</i> ^{-/-} cells and plasma membrane proteins identified by gene ontology (GO) analysis.....	28
--------------------------------------------------------------------------------------------------------------------------------------------------------------------------------------------------------------------------------------------------------------------------------	----

Chapter 1: Introduction

Autophagy

Autophagy is classically viewed as a catabolic pathway that sequesters cytoplasmic material in double-membraned organelles called autophagosomes, which are subsequently delivered to lysosomes for degradation¹. The canonical process of autophagy commences with the initiation of phagophore assembly. This process is mediated by the UNC51-like kinase (ULK) complex, which is composed of the autophagy-related proteins (ATGs) proteins ULK1/2, ATG13, FIP200, and ATG101. The ULK complex is responsible for activating a class III phosphatidylinositol 3-kinase (PI3K) complex, composed of Beclin 1 (ATG6), ATG14, and VPS34. Once activated by phosphorylation, the PI3K complex produces phosphatidylinositol triphosphate (PI3P), which acts as the initial membrane marker that recruits early autophagic effector proteins². Following initiation, the phagophore undergoes expansion. Expansion is mediated by two ubiquitin-like conjugation systems, which work together to induce the lipidation of microtubule-associated protein light chain 3 (LC3). These conjugation systems rely on multiple ATGs (including ATG3, ATG5, and ATG7) to complete the lipidation of LC3. As the phagophore expands, it is decorated with lipidated LC3 along its membrane³. LC3 is recognized by autophagy cargo receptors, such as p62, which promote the selective capture and engulfment of ubiquitinated proteins and organelles⁴. These autophagy cargo receptors bind LC3 via their LC3-interacting region (LIR) motifs, which promote the successful binding of the cargo receptors and their captured cargo within the autophagosomal membrane⁵. The autophagosome is then closed with the assistance of ATG2A and ATG2B¹⁰⁶, and subsequently trafficked to the lysosome. Upon fusion, lysosomal hydrolases degrade the inner membrane of the autophagosome along with the autophagosomal cargo contained inside⁷.

Overview of Secretory Autophagy

Autophagy is classically viewed as an autodigestive pathway in which cytosolic components are sequestered in autophagosomes and delivered to the lysosome for degradation. Recently, an increasing pool of studies have demonstrated that the autophagy pathway also facilitates cellular secretion. Autophagy-related proteins (ATGs) have been implicated in a diverse range of secretory functions, collectively termed secretory autophagy, including viral budding^{8,9}, the secretion of inflammatory cytokines and lysosomal contents^{10,11}, the exocytosis of autophagy cargo receptors during lysosome inhibition⁵, and the production of Evs^{8,13,14}. Recently, our lab described a secretory autophagy pathway termed LC3-dependent EV loading and secretion (LDELS) that facilitates the packaging of cytosolic cargoes, particularly RNA-binding proteins (RBPs), into EVs for secretion outside the cell¹³. This pathway utilizes a pool of LC3 localized at single membrane endosomes rather than double membrane autophagosomes. While our previous study focused on the requirement for this pathway in the secretion of soluble RBPs, we also observed a collection of proteins containing membrane-spanning regions that relied on this pathway for secretion. However, the role of secretory autophagy in the secretion of transmembrane proteins remains incompletely understood.

Extracellular Vesicles

Cells release a myriad of membrane vesicles, called extracellular vesicles (EVs), ranging in size and origin. This phenomenon is evolutionarily conserved across bacteria, plants, and human cells¹⁵⁻¹⁷. The secretion of EVs in mammalian cells was initially described as a means of eliminating unneeded transferrin receptor (TFRC) during reticulocyte maturation¹⁸. However, numerous studies have now shown that EVs are released in a highly regulated manner and are

capable of exchanging cargo between cells, including proteins and genetic material^{14,19,20}. EV biogenesis occurs when endosomal membranes undergo invagination to produce intraluminal vesicles (ILVs), thus forming multivesicular endosomes (MVEs). Recent research has detailed the active and specific incorporation of nucleic acid, lipid, and protein cargo into intraluminal vesicles (ILVs)^{13,21,22}. As the MVE fuses with the plasma membrane, these ILVs are released into the extracellular space as EVs^{19,23}.

The study of EVs has generated significant interest of late given their ability to evoke intercellular communication and non-cell autonomous activity in both normal homeostatic cell activity and pathological settings. For example, EVs reportedly contribute to the transport of secreted mRNA between cells and the transport of MHC II from dendritic cells to T cells^{21,24}. In pathological contexts, EVs have been shown to contribute to the suppression of the immune system by tumor cells²⁵, yet also protection against bacterial toxins²⁶. Despite these exciting functional implications, research into the mechanistic underpinnings of EV biogenesis and secretion has slowed. Furthermore, the extensive heterogeneity among EV populations has led to discourse concerning the contents and functional properties of EVs. Further research is needed to discern the specific molecular mechanisms involved in the biogenesis, loading, and secretion of EVs.

Transferrin Receptor

TFRC is responsible for iron uptake via the plasma glycoprotein transferrin (Tf)²⁷. Iron-bound Tf binds to TFRC, initiating clathrin-dependent internalization within an endocytic vesicle. The vesicle is then acidified causing the release of iron while Tf remains bound to TFRC. The Tf/TFRC complex is then recycled back to the cell surface where Tf is released into the extracellular space²⁸. TFRCs are likely expressed on all cells, but are highly expressed in immature erythroid cells and rapidly dividing cells, both normal and malignant. Over the past several

decades, studies have demonstrated the diverse roles of TFRC in a range of disease contexts including hematological disorders, neurodegenerative diseases, and cancer. Furthermore, experimental and clinical drugs and antibodies targeting TFRC have shown anti-tumor effects, thus TFRC has become a potential target for diagnosis and treatment of cancers²⁹. More recently, TFRC has been identified to be a specific marker of ferroptosis, a type of programmed cell death dependent on iron and characterized by the accumulation of lipid peroxides³⁰. Overall, we see research continuing to uncover new mechanisms by which TFRC plays a role in normal cellular functions and disease pathogenesis.

Interestingly, the term “exosome” was first coined in regards to EVs harboring TFRC released during reticulocyte maturation after being intraluminally bud within the multivesicular body^{18,31}. Despite TFRC being the first exosome marker ever reported^{31,32}, to date, the precise mechanisms directing the secretion of this transmembrane protein in extracellular vesicles have remained elusive. Furthermore, EVs containing TFRC have been connected to disease status and therapeutic applications in various contexts, including reticulocyte development and drug delivery³³⁻³⁵. In that sense, EV-associated TFRC and novel insights regarding the biogenesis of TFRC+ EVs represent an exciting opportunity for investigation.

Autophagy in Extracellular Vesicles Biogenesis

Autophagy has been implicated in the biogenesis and cargo loading of EVs. Specifically, autophagy-related proteins ATG5 and ATG16L1 have been shown to impact the overall production of exosomes while ATG7 did not¹⁴, suggesting the formation of autophagosomes and LC3 lipidation are not required for exosome biogenesis. MAP1LC3B (LC3) is an ATG8 orthologue that captures selective autophagy substrates by binding the LC3-interacting region (LIR) of substrates to the LIR-docking site (LDS) of LC3³⁶. LC3 was shown to localize to the

lumen of ILVs, the precursors of exosomes, although the biological function of this phenomenon was unclear¹⁴. Recently, our group showed that LC3 facilitates the selective cargo loading of vesicles before their release from the cell¹³. Among selectively loaded cargo substrates, TFRC emerged as a substrate strongly affected by ATG7 function. Collectively, these points suggest that ATG7 may play a role in the selective packaging of substrates such as TFRC into EVs. Nonetheless, the mechanism by which autophagy modulates TFRC loading into vesicles and release from the cell is incompletely understood.

Chapter 2: LC3-dependent EV loading and secretion (LDELS) promotes transferrin receptor secretion via extracellular vesicles

Summary

LC3-dependent EV loading and secretion (LDELS) is a secretory autophagy pathway in which the autophagy machinery facilitates the packaging of cytosolic cargos, such as RNA binding proteins, into extracellular vesicles (EVs) for secretion outside of the cell. Here, we identify transferrin receptor (TFRC), one of the first proteins uncovered to be secreted via EVs, previously termed exosomes, as a transmembrane cargo of the LDELS pathway. Similar to other LDELS targets, TFRC secretion via EVs genetically requires components of the LC3-conjugation machinery but is independent of other *ATGs* involved in classical autophagosome formation. Furthermore, the packaging and secretion of this transmembrane protein into EVs depends on multiple ESCRT pathway components and the small GTPase RAB27A. Based on these results, we propose that the LDELS pathway promotes the TFRC incorporation into EVs and its secretion outside the cell.

Introduction

While autophagy pathway components (*ATGs*) are essential for the lysosomal degradation of cytosolic material, they also play important roles in non-autophagic processes, including cellular secretion^{13,37}. Genetic loss-of-function studies demonstrate that *ATGs* are required for the efficient secretion of inflammatory cytokines¹⁰, release of bactericidal enzymes and tissue repair factors³⁸, exocytosis of autophagy cargo receptors during lysosome inhibition¹² and extracellular vesicle (EV) secretion^{8,14}. Recently, we described a secretory autophagy pathway termed LC3-dependent EV loading and secretion (LDELS) that facilitates the packaging of cytosolic cargoes, most notably, RNA-binding proteins (RBPs) into EVs for secretion outside the cell¹³. This pathway utilizes a pool of LC3 localized at single membrane endosomes rather than double membrane autophagosomes. Hence, LDELS is akin to other autophagy-related pathways involving the conjugation of ATG8 to single membranes (CASM)³⁹, including LC3-associated endocytosis (LANDO)⁴⁰. In addition, endosomal microautophagy (eMI) has been implicated in the turnover of cytosolic components and integral membrane proteins. In eMI, cytosolic proteins are engulfed via intraluminal budding that mediated the endosomal sorting complexes required for transport (ESCRT) machinery, thereby resulting in cargo incorporation into intraluminal vesicles (ILVs)⁴¹⁻⁴⁴.

Because LANDO and eMI both play important roles in the trafficking and clearance of membrane proteins, we hypothesized that the LDELS may similarly specify integral membrane proteins for EV loading and secretion. Here, we define a previously unrecognized role for the autophagy machinery in EV-mediated secretion of the integral membrane protein transferrin receptor (TFRC). Similar to LDELS secretion of RNA-binding proteins, TFRC secretion requires the LC3-conjugation machinery but not other *ATGs* necessary for autophagosome formation. We

also demonstrate that ATG8 family members directly bind to the cytosolic domain of TFRC, which may contribute to the packaging of this transmembrane protein into EVs. Finally, we delineate that TFRC secretion via EVs functionally requires ESCRT pathway components and the small GTPase RAB27A, which have both been previously implicated in EV biogenesis and cargo loading^{19,45,46}. Given the similarities between the mechanisms of TFRC secretion and EV-mediated release of RBPs, we propose that the LDELS pathway promotes the extracellular secretion of TFRC via EVs.

Results

ATG7 is genetically required for the secretion of transmembrane proteins in extracellular vesicle and particle (EVP) fractions.

We recently described a secretory autophagy pathway termed LDELS that employs the LC3-conjugation machinery to load RNA binding proteins and small RNAs into EVs¹³. To gain a broader understanding of putative substrates and cargoes secreted by the LDELS pathway, we further scrutinized the Tandem Mass Tag (TMT)-based quantitative proteomic data from this study. We focused on identifying membrane proteins enriched in the 100,000g conditioned media fractions (100K) from wild-type (WT) cells versus those deficient for *ATG7* or *ATG12*. Importantly, although these 100K fractions are enriched for small EVs (exosomes), they contain a broader array of nanoparticles and proteins, collectively termed extracellular vesicles and particles (EVPs)⁴⁷. From a total of 1,071 proteins enriched in EVPs from WT cells versus *ATG7*-deficient cells or *ATG12*-deficient cells, 30 proteins were classified as plasma membrane proteins by gene ontology analysis (GO) and also contained membrane-spanning regions (Figure 2.1A, Supplemental Figure 2.1, Supplemental Table 2.1). Amongst these, the transmembrane proteins TFRC, IGF2R, and LAMP2, stood out on the basis of their high quantitative mass spectrometry intensity values, an indication of relative peptide abundance (Table S2.1). Interestingly, these proteins have all previously been detected in EVs⁴⁸⁻⁵⁰. In fact, TFRC was the first protein identified in EVs^{18,31} and its secretion is proposed as a crucial step in the maturation of reticulocytes into erythrocytes⁵¹.

To corroborate our prior proteomic data, we first evaluated the secretion of TFRC, IGF2R, and LAMP2 in EVP fractions from WT and *ATG7* deficient cells via immunoblotting (100K, Figure 2.1B, C). These analyses confirmed *ATG7* to be necessary for the efficient release of TFRC,

IGF2R, and LAMP2 in EVPs, with TFRC showing the most significant reduction in secretion upon loss of *ATG7*. Because cells secrete many different types of EVs and nanoparticles including large EVs bud from the plasma membrane (microvesicles, ectosomes) and small EVs that originate from the endosomal system (exosomes), we next performed serial differential centrifugation of conditioned media to determine whether TFRC was enriched in specific fractions (Figure 2.1D). Although 10,000g (10K) fractions corresponding to large EVs contained modest levels of TFRC, this membrane protein was highly enriched, along with LC3-II in small EVP populations isolated at 100,000g (100K) (Figure 2.1E, F). Further purification of 100,000g fractions via linear sucrose density gradient flotation demonstrated that TFRC robustly co-fractionates with LC3 and the EV-associated tetraspanin CD63 at buoyant densities consistent with small EVs (Figure 2.1G, H). Finally, we employed antibodies targeting the extracellular domain of CD63 or TFRC to specifically immuno-isolate EVs from the 100K fraction of conditioned media. Immunoblotting of these immuno-isolated EVs revealed that LC3 specifically co-purified with CD63 and TFRC, but not immunoglobulin controls (Figure 2.1I), suggesting that LC3 resides within CD63⁵¹TFRC⁵¹ EVs. Overall, these results demonstrate that TFRC is secreted extracellularly in association with small EVs via an ATG7-dependent mechanism.

TFRC secretion in EVs requires the LC3-conjugation pathway but is independent of other components involved in classical autophagosome formation.

To determine whether autophagy pathway components are generally required for TFRC release in EVPs, we examined the secretion of this transmembrane protein in cells deficient for the early initiation factors *ATG14* and *RB1CC1/FIP200* as well as *ATG7*. Potential differences in EV production among these *ATG* deficient cells¹³ were controlled for by normalizing the protein

content of EV lysates. Importantly, analyses of 100K EVP fractions revealed that in contrast to *ATG7*, the initiation factors *ATG14* and *RBICC1/FIP200* were completely dispensable for TFRC secretion in EVPs; rather, disruption of these initiation components enhanced TFRC secretion (Figure 2.2A, B). Additionally, EVP secretion of TFRC and LC3-II was reduced upon siRNA depletion of the LC3-conjugation components *ATG3* and *ATG5* (Figure 2.2C, D). These results support that TFRC secretion in EVPs, similar to the RNA-binding protein cargo of the LDELS pathway, requires LC3 processing and lipidation but is independent of other components necessary for classical degradative autophagy. Autophagic flux assays demonstrated that TFRC did not accumulate within cells as a result of impaired lysosomal acidification in nutrient replete conditions or following starvation-induced autophagy (Figure 2.2E). When taken together with our quantitative mass spectrometry data (Figure 2.1A, Supplemental Figure 2.1), TFRC secretion via EVPs requires LC3 processing and lipidation but is independent of other mediators of classical degradative autophagy. These findings are in line with our previous observations for RNA-binding proteins secreted via the LDELS pathway¹³.

Remarkably, pharmacological inhibition of lysosomal acidification using Bafilomycin A (BafA1) enhanced TFRC and LC3 secretion in 100K EVP fractions (Figure 2.2F, G). We recently described a pathway, called secretory autophagy during lysosome inhibition (SALI), which promotes the secretion of autophagy cargo receptors via extracellular nanoparticles in response to endolysosomal dysfunction¹². However, the robust secretion of TFRC in cells lacking *ATG14* and *RBICC1*, both of which are functionally required for SALI, argues against a major role for this pathway in extracellular release of TFRC. Overall, based on these results, we propose that LDELS or an LDELS-like pathway promotes the extracellular secretion of TFRC via EVs.

ATG8 family proteins bind TFRC via a cytoplasmic domain LIR motif.

In the LDELS pathway, LC3 directly binds to and mediates the packaging of specific RBP cargoes into EVs, such as scaffold-attachment factor B (SAFB), for secretion outside the cell¹³. To determine whether TFRC is packaged into EVs through similar mechanisms, we first tested for TFRC interaction with the various ATG8 family orthologs. Co-immunoprecipitation assays revealed that TFRC specifically bound to all ATG8 orthologs (Figure 2.3A), showing a preference for interaction with LC3A, LC3B, and LC3C. ATG8 proteins frequently bind their substrates via LIR (LC3-interacting region) motifs⁵². Because LC3 is localized to the interior of EVs¹³, we postulated that the cytoplasmic tail of TFRC would be accessible for interaction with LC3. Bioinformatic analyses⁵³ predicted a LIR motif within the cytoplasmic tail of TFRC coinciding with its YTFR internalization motif, a region previously shown to directly interact with the ATG8 ortholog GABARAP⁵⁴ (Figure 2.3B). Therefore, we mutated this putative LIR within a soluble, recombinant protein comprising the cytoplasmic N-terminal domain of TFRC fused to luciferase. Simultaneous mutation of tyrosine-20 and phenylalanine-23 to alanine (Y20A, F23A; AA) within the TFRC cytoplasmic domain disrupted binding to both LC3B and GABARAP (Figure 2.3C), as well as the other ATG8 family members (Supplemental Figure 2.2A). This suggests that LC3 at least partly interacts with TFRC through a LIR in the cytoplasmic domain of this transmembrane protein. To evaluate the impact of this LIR mutation on secretion, we generated cells that stably express full length TFRC (TFRC-HA; WT) or mutants that either contain substitutions in critical LIR residues (TFRC⁵⁴-HA; AA) or are deleted for all but four amino acids of the cytoplasmic domain (TFRC Δ 3-59-HA; Δ CD). Surprisingly, neither the LIR mutant nor the cytoplasmic domain truncation mutant significantly affected TFRC secretion (Figure 2.3D, E). This suggested that regions outside of the cytoplasmic domain of TFRC may also facilitate interactions with LC3, a

notion further supported by the binding of the TFRC cytoplasmic domain truncation mutants to LC3B and GABARAP (Supplemental Figure 2.2B). In support of this, utilizing antibodies specifically directed against the epitopes located in either the cytoplasmic or extracellular domains of TFRC, we determined that both domains of TFRC exhibited partial protease protection when EVs were treated with trypsin in the absence of detergent (Figure 2.3F). Importantly, these results are consistent with TRFC being incorporated as a transmembrane protein into EVs secreted via LDELS. At the same time, they broach that TFRC exists in both canonical and reversed topologies within the membranes of EVs. Indeed, recent studies have revealed a number of transmembrane proteins exhibiting unconventional or reversed topologies in EV membranes⁵⁵. Based on these results, we postulate that the cytoplasmic LIR promotes TFRC interaction with LC3. Nevertheless, TRFC existing in an unconventional or reversed topology may allow LC3 to potentially interact with cryptic LIRs of the TFRC extracellular domain (Figure 2.3B). Alternatively, other features of the TFRC extracellular domain may facilitate packaging and secretion outside the cell.

ESCRT machinery and RAB27A promotes TFRC loading and secretion via EVs.

EV biogenesis occurs within the endosomal system as endosomal membranes undergo invagination to produce intraluminal vesicles (ILVs), thus forming multivesicular endosomes (MVEs)⁵⁶. In our studies of RBP secretion via LDELS, the biogenesis of ILVs via the LDELS pathway functionally required neutral sphingomyelinase 2 (nSMase2), which converts sphingomyelin to ceramide to induce inward budding at the MVB⁵⁷. Thus, we asked whether nSMase2 was similarly required for the secretion of TFRC in EVs. However, treatment with the nSMase2 catalytic inhibitor GW4869 did not significantly reduce TFRC secretion, arguing against a specific requirement for nSMase2 (Figure 2.4A, B). We next assessed the role of ESCRT

machinery in EV-mediated secretion of TFRC, employing short interfering RNAs (siRNAs) to deplete key ESCRT components including PDCD6IP/ALIX, HGS and TSG101 and evaluate the impact on TFRC release. Genetic depletion of PDCD6IP and HGS impaired both TFRC and LC3-II secretion in EVs, whereas the loss of TSG101 had a negligible impact (Figure 2.4C, D). Taken together, these data suggest that TFRC incorporation into ILVs functionally requires an ESCRT-dependent intraluminal budding pathway. Upon incorporation of resident cargo within ILVs at the MVE, fusion of these MVEs with the plasma membrane is required for secretion outside of the cell⁴⁵. RAB27A, a small GTPase of the Rab superfamily, has been implicated in the docking of MVBs at the plasma membrane to release EVs^{46,58}. Accordingly, we examined the role of RAB27A in the release of EVs containing TFRC. Short hairpin RNAs (shRNAs) targeting *RAB27A* strongly suppressed both TFRC and LC3-II secretion (Figure 2.4E, F). Thus, RAB27A is functionally required for the secretion of TFRC and LC3-II. Altogether, these results suggest that, in contrast to the nSMase2-dependent release of RNA-binding proteins, ESCRT- and RAB27A-dependent mechanisms functionally contribute to EV loading and secretion of TFRC via the LDELS pathway. Furthermore, by uncovering a genetic requirement for RAB27A in the EV secretion of both TFRC and LC3-II, our results corroborate our originally proposed model that EVs generated via the LDELS pathway originate from MVEs or late endosomes, rather than via direct outward budding from the plasma membrane^{13,59}.

Discussion

Interestingly, the term “exosome” was first coined in regards to EVs harboring TFRC released during reticulocyte maturation after being intraluminally bud within the multivesicular body^{18,31}. Despite TFRC being the first exosome marker ever reported^{31,32}, to date, the precise mechanisms directing the secretion of this transmembrane protein in extracellular vesicles have

remained elusive. Here, we demonstrate that the LC3-conjugation machinery functional contributes to the EV-mediated secretion of TFRC. In addition, TFRC secretion requires specific ESCRT-associated components including PDCD6IP and HGS. Previously described LDELS substrates, such as the RNA-binding proteins SAFB and HNRNPK, utilized an nSMase2-dependent mechanism for secretion, suggesting that LDELS substrates may have differing and substrate-specific mechanisms of intraluminal budding.

Overall, our results here expand the protein cargo secreted via LDELS beyond our original description of RNA binding proteins by demonstrating that this secretory autophagy pathway mediates the incorporation of transmembrane proteins into EVs released outside of the cell. An important unanswered question is whether and how the LDELS modulates disease progression and physiological functions *in vivo*. In this regard, EVs containing TFRC have been connected to disease status and therapeutic applications in various contexts, including reticulocyte development and drug delivery³³⁻³⁵. Determining whether and how TFRC secretion via LDELS influences reticulocyte development and more broadly regulates cellular iron uptake and homeostasis remains an important topic for future study.

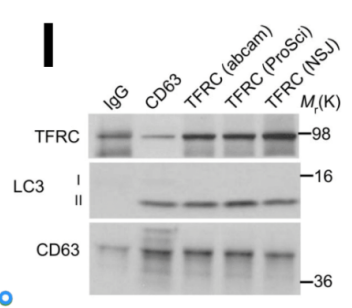
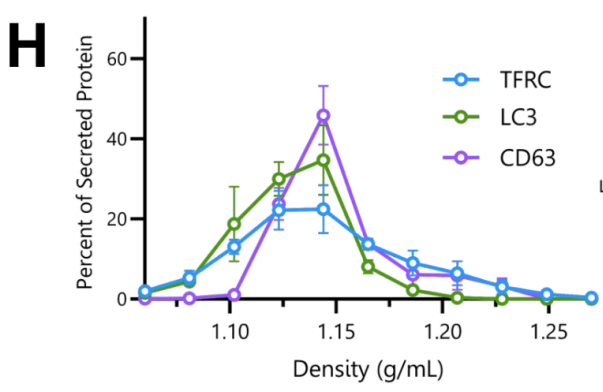
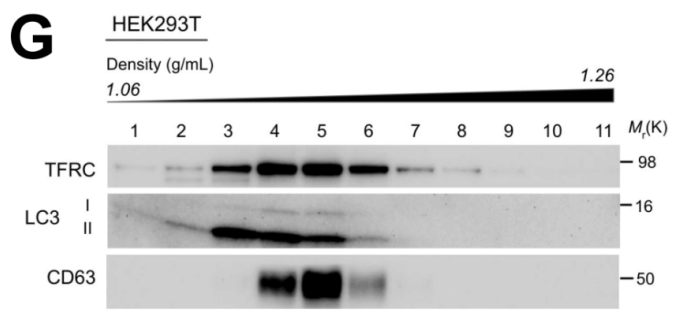
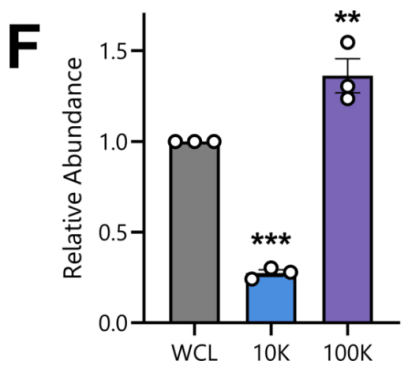
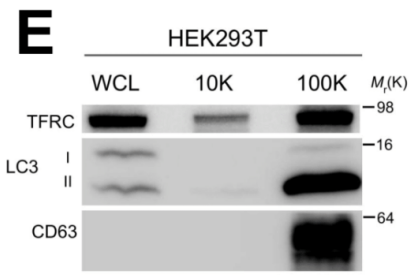
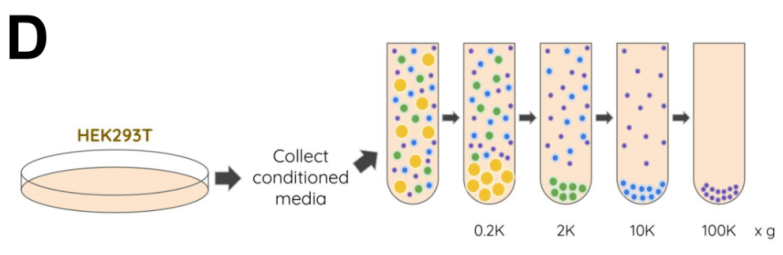
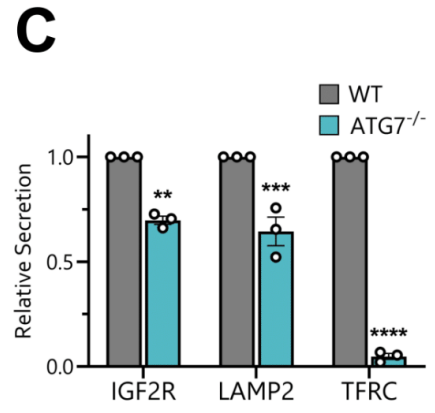
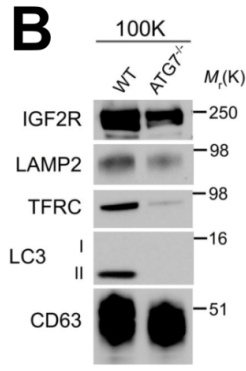
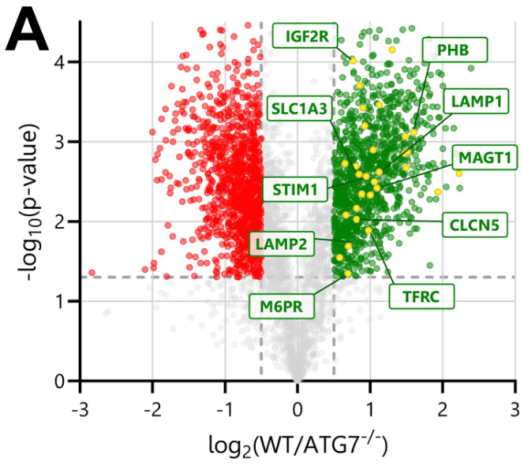


Figure 2.1: *ATG7* is genetically required for the secretion of transmembrane proteins via extracellular vesicles.

(A) Volcano plot of the proteins identified in 100,000g EVP-enriched fractions for WT and *ATG7*^{-/-} HEK293T cells quantified by TMT mass spectrometry in Leidal et al. 2020. TMT-labeled proteins are plotted according to their $-\log_{10} P$ values as determined by two-tailed t-test and log₂ fold enrichment (WT/*ATG7*^{-/-}; n = 4). Gray dots: proteins not relatively enriched in EVPs from WT or *ATG7*^{-/-} cells identified with $P > 0.05$ and/or log₂ fold change between -0.5 and 0.5 . Green dots: proteins significantly enriched in EVs from WT cells relative to *ATG7*^{-/-} cells. Red dots: proteins significantly enriched in EVs from *ATG7*^{-/-} cells relative to WT cells. Yellow dots: plasma membrane proteins identified by gene ontology (GO) analysis. (B) 100,000g EV fractions (100K) from WT and *ATG7*^{-/-} cells were collected, normalized for protein concentration, and immunoblotted to detect the endogenous levels of the indicated proteins (n = 3). (C) Quantification of TFRC levels in EVs from *ATG7*^{-/-} (cyan) cells relative to WT (gray) (mean \pm s.e.m.; n = 3). Statistical significance calculated by one-way ANOVA coupled with Tukey's post hoc test. (D) Schematic detailing the differential centrifugation protocol employed to isolate small EVP-enriched fractions from cell cultures. (E) Whole cell lysate (WCL) and fractionated conditioned media (CM) collected from serum-starved HEK293Ts. CM was subjected to serial differential ultracentrifugation to recover large EVs (10,000g; 10K) and small EVPs (100,000g; 100K). Equal volumes of fractionated CM were probed for the indicated proteins alongside WCL normalized to protein content of the 100K fraction (n = 3). (F) Quantification of TFRC in the indicated fractions of CM from serum-starved cells relative to WCL (mean \pm s.e.m.; n = 3). Statistical significance was calculated by one-way ANOVA with Tukey's post hoc test. (G) EVs from CM separated via linear sucrose density gradient ultracentrifugation, fractionated and immunoblotted to detect TFRC, LC3, and the EV marker protein CD63 (n = 3). (H) Percent of total secreted TFRC, LC3, and CD63 detected in individual linear sucrose gradient fractions (mean \pm s.e.m.; n = 3). (I) Representative immunoblots of EVs immunopurified from concentrated CM fractions using a normal mouse IgG isotype control, an antibody against the tetraspanin CD63, and antibodies against TFRC from three independent manufacturers (n = 3).

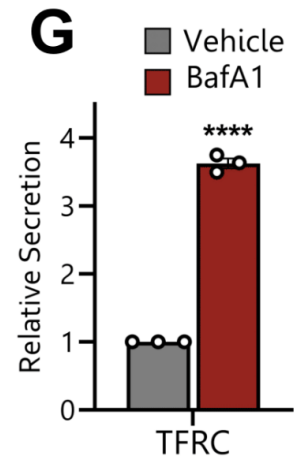
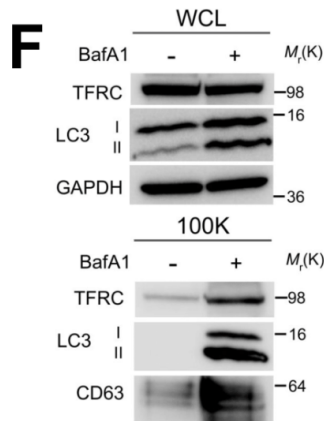
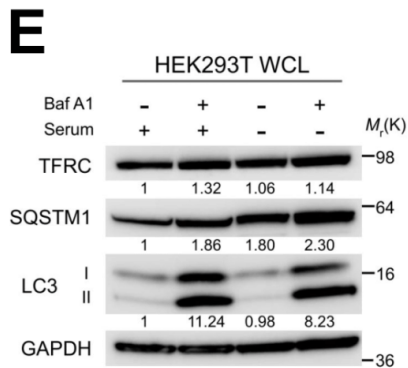
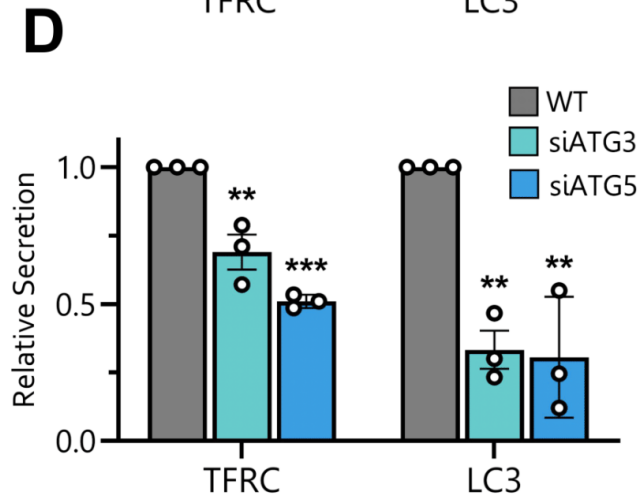
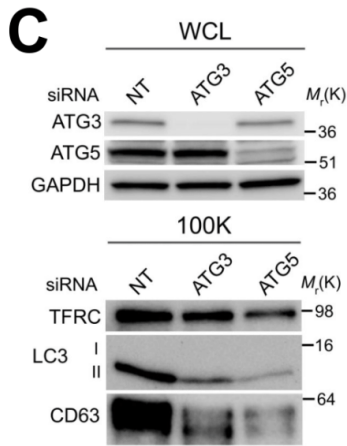
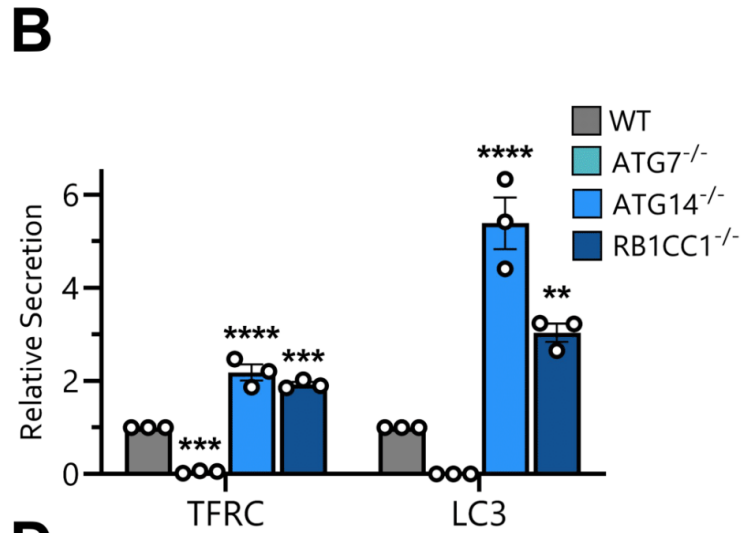
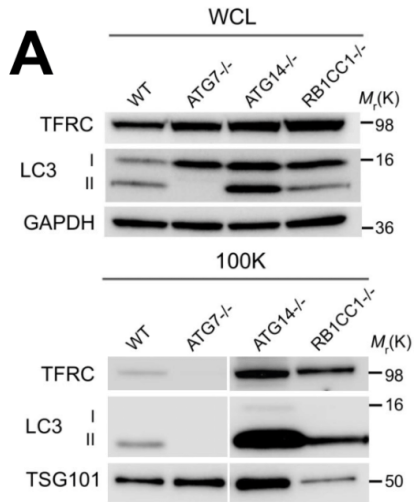


Figure 2.2: Transferrin receptor (TFRC) secretion in EVs requires the LC3-conjugation pathway but is independent of other components mediating classical autophagosome formation.

(A) Whole cell lysate (WCL; top) and 100,000g EV fractions (100K; bottom) from the indicated cell types were collected, normalized for protein concentration and immunoblotted to detect the endogenous levels of the indicated proteins ($n = 3$). Individual lanes shown are from the same representative immunoblot. (B) Quantification of TFRC and LC3-II levels in EVs from the indicated *ATG*-deficient cell lines relative to WT (mean \pm s.e.m.; $n = 3$). Statistical significance calculated by one-way ANOVA coupled with Tukey's post hoc test. (C) WCL (top) and 100K fractions (bottom) from equal numbers of wild-type HEK293T cells transfected with non-targeting (NT) control siRNA or siRNAs targeting *ATG3* and *ATG5* and immunoblotted for the indicated proteins ($n = 3$). (D) Quantification of TFRC and LC3-II levels in EV fractions from cells treated with siRNAs targeting the indicated proteins relative to cells treated with NT control siRNA (mean \pm s.e.m.; $n = 3$). Statistical significance calculated by one-way ANOVA coupled with Tukey's post hoc test. (E) HEK293Ts cultured in serum-starved or complete media and treated with DMSO or 20 nM Bafilomycin A1 (Baf A1) for 18 h were then lysed and immunoblotted for TFRC and the indicated proteins ($n = 3$). Quantifications of TFRC, SQSTM1/p62, and LC3-II relative protein levels (values normalized to GAPDH) in WCLs from cells cultured in the indicated conditions relative to complete, vehicle-treated media are shown. (F) WCL (top) and 100K fractions (bottom) from serum-starved HEK293Ts treated with vehicle or 20 nM BafA1 for 16h were collected and immunoblotted to detect the indicated proteins ($n = 3$). (G) Quantification of TFRC in EV fractions from BafA1-treated cells relative to vehicle control (mean \pm s.e.m.; $n = 3$). Statistical significance calculated by an unpaired two-tailed t-test.

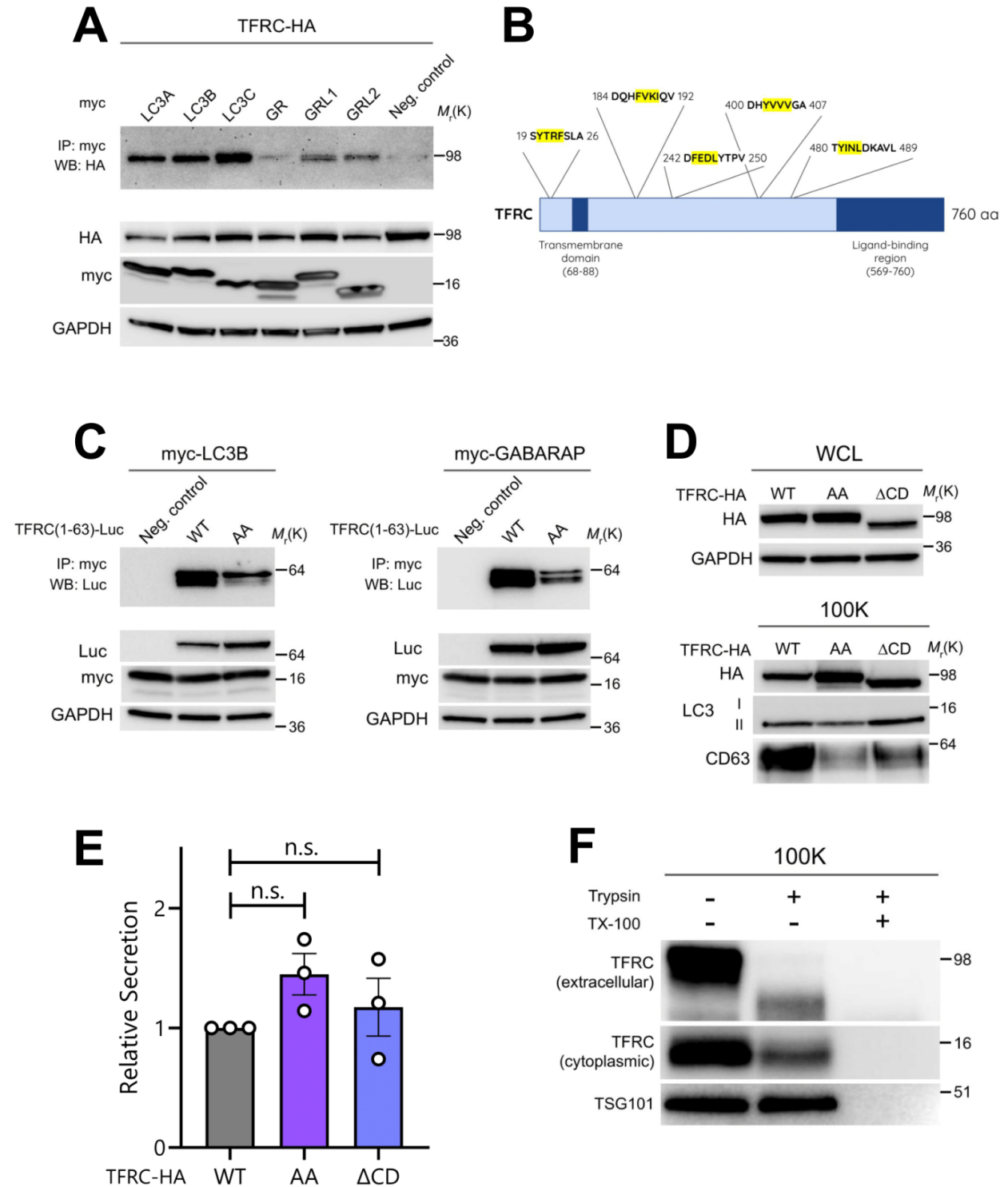


Figure 2.3: ATG8 family proteins bind TFRC via a cytoplasmic domain LIR motif.

(A) HEK293T cells co-transfected with HA-tagged TFRC and myc-tagged LC3A, LC3B, LC3C, GABARAP (GR), GABARAPL1 (GRL1), GABARAPL2 (GRL2) were lysed,

immunoprecipitated with anti-myc antibody and immunoblotted with the indicated antibodies (n = 3). **(B)** Domain map and the putative LIRs of TFRC highlighted in yellow. **(C)** Cells co-transfected with luciferase-tagged cytoplasmic domain from WT TFRC(1-63) or mutant TFRC(1-63)^{Y20AF23A} (AA) along with myc-tagged LC3B or myc-tagged GABARAP as indicated. Cells were lysed, immunoprecipitated with anti-myc antibody and immunoblotted with the indicated antibodies (n = 3). **(D)** WCL (top) and 100K fractions (bottom) from cells stably expressing HA-tagged WT TFRC, mutant TFRC^{Y20AF23A} (AA), or truncated TFRC lacking the cytoplasmic domain (TFRC Δ 3-59; Δ CD) were immunoblotted for the indicated markers (n = 3). **(E)** Quantification of TFRC-HA in EVs from equal numbers of HEK293T cells expressing HA-tagged WT TFRC, mutant TFRC^{Y20AF23A} (AA), or truncated TFRC lacking the cytoplasmic domain (TFRC Δ 3-59; Δ CD) (mean \pm s.e.m.; n = 3). Statistical significance calculated by one-way ANOVA coupled with Tukey's post hoc test. **(F)** Representative immunoblots of the indicated proteins from untreated EVs and EVs incubated with 100 μ g ml⁻¹ trypsin and/or 1% Triton X-100 (TX-100) for 30 min at 4 °C (n = 3).

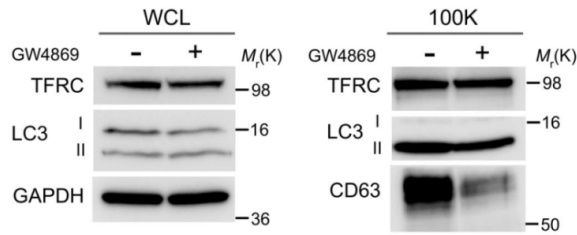
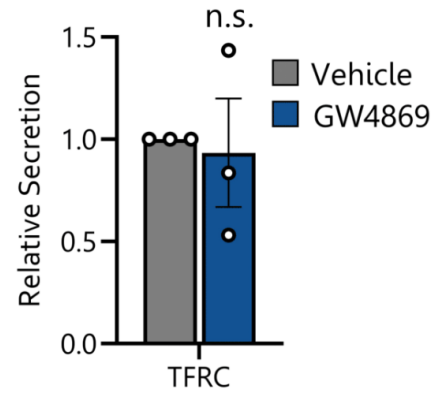
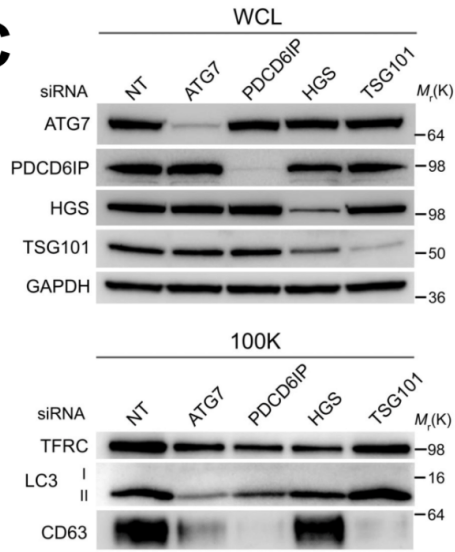
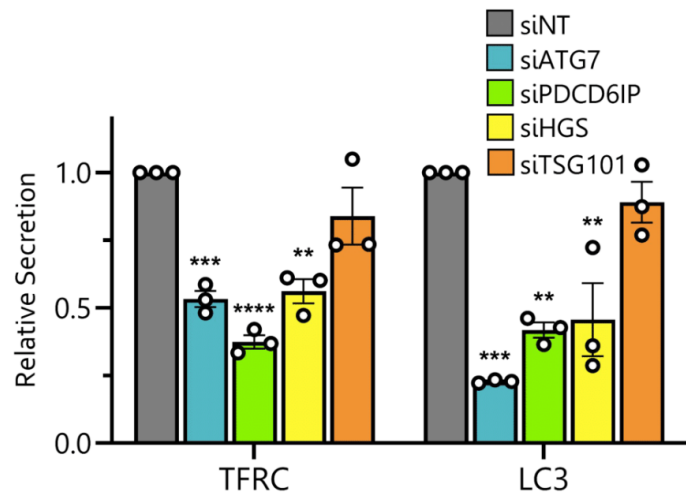
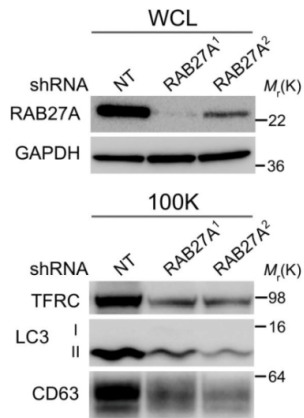
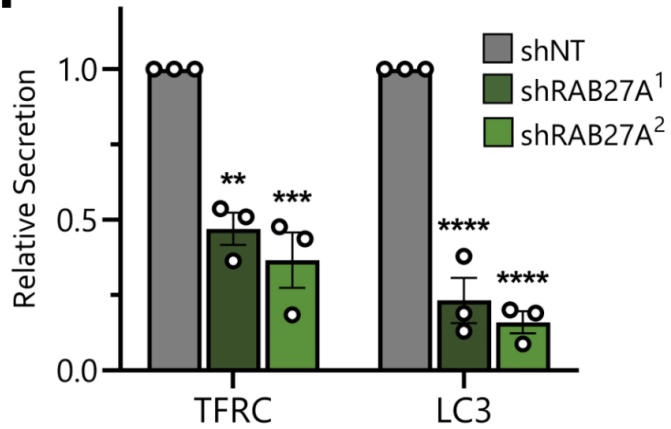
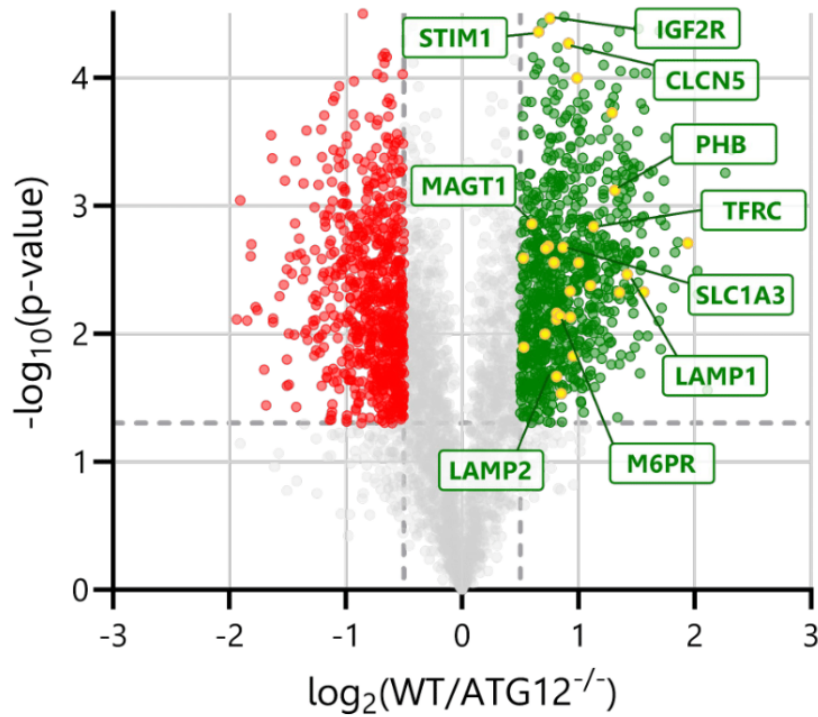
A**B****C****D****E****F**

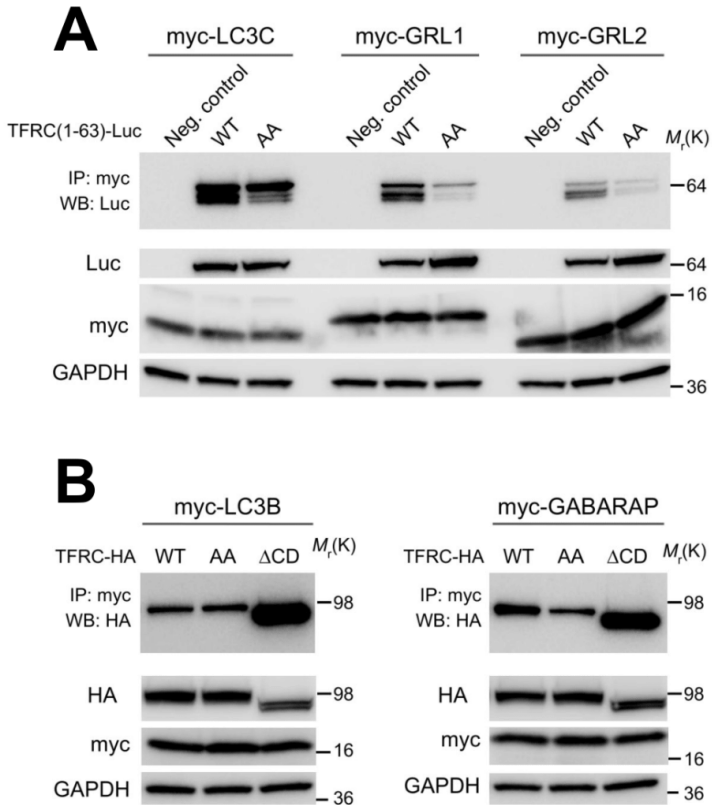
Figure 2.4: ESCRT machinery and RAB27A promotes TFRC loading and secretion via EVs.

(A) Whole cells lysates (WCL; left) and EV lysates (100K; right) from cells treated in the absence or presence of 5 μ M GW4869 for 24 h and immunoblotted for the indicated proteins (n = 3). (B) Quantification of TFRC levels in EV fractions from GW4869-treated cells relative to vehicle control (mean \pm s.e.m.; n = 3). Statistical significance calculated by an unpaired two-tailed t-test. (C) WCL (top) and 100K fractions (bottom) from equal numbers of wild-type HEK293T cells transfected with non-targeting (NT) control siRNA or siRNAs targeting *ATG7*, *PDCD6IP*, *HGS*, and *TSG101* and immunoblotted for the indicated proteins (n = 3). (D) Quantification of TFRC and LC3-II levels in EV fractions from cells treated with siRNAs targeting the indicated proteins relative to cells treated with NT control siRNA (mean \pm s.e.m.; n = 3). Statistical significance calculated by one-way ANOVA coupled with Tukey's post hoc test. (E) WCL (top) and 100K fractions (bottom) from equal numbers of cells stably expressing non-targeting (NT) shRNA or shRNAs that deplete RAB27A immunoblotted for indicated proteins (n = 3). (F) Quantification of TFRC and LC3-II levels in EV fractions from RAB27A depleted cells (shRAB27A) relative to controls expressing NT shRNA. (mean \pm s.e.m.; n = 3).



Supplementary Figure 2.1: *ATG12* is genetically required for the secretion of transmembrane proteins via extracellular vesicles.

Volcano plot of the proteins identified in 100,000g EVP-enriched fractions for WT and *ATG12*^{-/-} HEK293T cells quantified by TMT mass spectrometry in Leidal et al. 2020. TMT-labeled proteins are plotted according to their $-\log_{10}$ P values as determined by two-tailed t-test and \log_2 fold enrichment ($\text{WT}/\text{ATG12}^{-/-}$; n = 4). Gray dots: proteins not relatively enriched in EVPs from WT or *ATG12*^{-/-} cells identified with P > 0.05 and/or \log_2 fold change between -0.5 and 0.5. Green dots: proteins significantly enriched in EVs from WT cells relative to *ATG12*^{-/-} cells. Red dots: proteins significantly enriched in EVs from *ATG12*^{-/-} cells relative to WT cells. Yellow dots: plasma membrane proteins identified by gene ontology (GO) analysis.



Supplementary Figure 2.2: Deletion of the TFRC cytoplasmic domain or mutation of the cytoplasmic domain LIR is not sufficient to disrupt TFRC co-immunoprecipitation with ATG8 family proteins.

(A) Cells co-transfected with luciferase-tagged cytoplasmic domain of WT TFRC(1-63) or mutant TFRC(1-63)^{Y20AF23A} (AA) along with myc-tagged LC3C, myc-tagged GABARAPL1 (GRL1), or myc-tagged GABARAPL2 (GRL2). Indicated cells were lysed, immunoprecipitated with anti-myc antibody and immunoblotted with the indicated antibodies (n = 3). (B) Cells co-transfected with HA-tagged WT TFRC, mutant TFRC^{Y20AF23A} (AA), or truncated TFRC lacking the cytoplasmic domain (Δ CD, TFRC Δ 3-59) and myc-tagged LC3B or myc-tagged GABARAP were lysed, immunoprecipitated with anti-myc antibody and immunoblotted with the indicated antibodies (n = 3).

Supplementary Table 2.1: Proteins identified from quantitative proteomic datasets of EVP fractions collected from control (WT) vs. *ATG7*^{-/-} or *ATG12*^{-/-} cells and plasma membrane proteins identified by gene ontology (GO) analysis.

Original TMT quantitative proteomic datasets were previously generated and described in detail in Leidal et al., 2020.

Experimental Procedures

Cell culture

HEK-293T (ATCC, CRL-3216) were cultured in Dulbecco's Modified Eagle Medium (DMEM), high glucose, pyruvate (Gibco, 11995040) supplemented with 10% fetal bovine serum (FBS) (Atlas Biologicals, F-0500-D), and 100 units/mL penicillin and 100 μ L/mL streptomycin (Gibco, 14140163). This cell line was tested for mycoplasma contamination (SigmaAldrich, MP0035).

Unless otherwise indicated, CM and EV preparations were collected following 24 h incubation in DMEM containing all supplements except FBS. For autophagy flux assays, cells were incubated with 20 nM bafilomycin A1 (Sigma, B1793) as indicated for 16 h before CM collection and lysis. Treatment with 5 μ M GW4869 (Cayman, 13127) or vehicle (dimethylsulfoxide) (Sigma Aldrich, 472301) in serum-free DMEM for 24 h was used to inhibit nSMase activity.

Plasmid constructs

The following vectors are available or were obtained from Addgene: pcDNA3.2/DEST/hTfR-HA (69610; Robin Shaw), pBABE-puro-GFP-LC3 (22405; Jayanta Debnath). To generate pcDNA3-TFRC-HA, TFRC-HA was amplified with flanking primers (Fwd: atcggaattcgccaccatgatggatcaagctagatcagcat; Rev: atgcgcggccgcttacgcgtaactctgggacgtcg) from pcDNA3.2/DEST/hTfR-HA and sub-cloned into pcDNA3 between the EcoRI and NotI sites. To generate pcDNA3-TFRC(Δ 3-59)-HA, TFRC-HA was amplified from pcDNA3.2/DEST/hTfR-HA with the same reverse primer as above but with a forward primer containing the first two amino-terminal codons of TFRC (Met-Met) in its overhang and sequence alignment beginning at Lys-60 (Fwd: atcggaattcgccaccatgatgaaaaggtgtagtggaagtatct). This product was then sub-cloned

into pcDNA3 between the EcoRI and NotI sites. To generate pcDNA3-TFRC^{Y20AF23A}-HA, site-directed mutagenesis of pcDNA3-TFRC-HA was performed via QuikChange PCR. First, overlapping primers carrying the desired Y20A mutation (Fwd: gaaccattgtcagctaccgggttcag; Rev: ctgaaccgggtagctgacaatggcttc) were used to amplify pcDNA3-TFRC-HA and templated plasmid was eliminated via DpnI digestion. Subsequently, individual clones were sequenced to verify mutagenesis of the desired site. This process was then repeated with the pcDNA3-TFRC^{Y20A}-HA construct and overlapping primers carrying F23A mutation (Fwd: gtcagctaccgggccagcctggctcggc; Rev: gccgagccaggctggcccggttagctgac) in order to generate pcDNA3-TFRC^{Y20AF23A}-HA.

To generate pcDNA3-TFRC(1-63)-Luc, luciferase (Luc) was amplified with flanking primers (Fwd: atcggaattcatggaagacgcaaaaacataaagaaaggc; Rev: atcggcgccgcctactattacaattggactttccgcccttctgg) from pRetroX-Tight-Pur-Luc (Takara 632104) and sub-cloned into pcDNA3 between EcoRI and NotI sites to generate pcDNA3-Luc. Subsequently, TFRC(1-63) was amplified with flanking primers (Fwd: actgaagcttgccaccatgatggatcaagctagatca; Rev: actgggatcccactacaccttttggttttgtgacattg) from pcDNA3-TFRC-HA and sub-cloned into pcDNA3-Luc between the HindIII and BamHI sites. To generate pcDNA3-TFRC(1-63)^{Y20AF23A}-Luc, the same process was repeated as above this time using pcDNA3-TFRC^{Y20A}-HA as template DNA for amplification with the same flanking primers, thus generating pcDNA3-TFRC(1-63)^{Y20A}-Luc. Subsequently, site-directed mutagenesis of pcDNA3-TFRC(1-63)^{Y20A}-Luc was performed via QuikChange PCR. Overlapping primers carrying the desired F23A mutation (Fwd: gtcagctaccgggccagcctggctcggc; Rev: gccgagccaggctggcccggttagctgac) were used to amplify pcDNA3-TFRC(1-63)^{Y20A}-Luc and

template plasmid was eliminated via DpnI digestion. Individual clones were sequenced to verify mutagenesis of the desired site.

To generate pBABE-puro-TFRC-HA, TFRC-HA was amplified with flanking primers (Fwd: actgaccggtgccaccatgatggatcaagctagatca; Rev: actggtcgacttacgcgtaatctgggacgtcg) from pcDNA3-TFRC-HA and sub-cloned into pBABE-puro-GFP-LC3 between AgeI and Sall, effectively replacing the GFP-LC3 open reading frame. To generate pBABE-puro-TFRC^{Y20AF23A}-HA, the above was repeated, this time using pcDNA3-TFRC^{Y20AF23A}-HA as template DNA for amplification. To generate pBABE-puro-TFRC Δ 3-59-HA, TFRC(Δ 3-59)-HA was amplified with flanking primers (Fwd: actgaccggtgccaccatgatgaaaaggtgtagtgga; Rev: actggtcgacttacgcgtaatctgggacgtcg) from pcDNA-TFRC Δ 3-59-HA and sub-cloned into pBABE-puro-GFP-LC3 as above. All constructs were verified by sequencing.

RNA interference

For transient siRNA-mediated knockdown, cells were transfected with siRNA using DharmaFECT no. 1 (Horizon Discovery, T-2001-03) according to the manufacturer's instructions. ON-TARGETplus smart pools against *ATG7* (10533; Horizon Discovery, L-020112-00-0005), *ATG3* (64422; Horizon Discovery, L-015375-00-0005), *ATG5* (9474; Horizon Discovery, L-004374-00-0005), *PDCD6IP* (ALIX) (10015; Horizon Discovery, L-004233-00-0005), *TSG101* (7251; Horizon Discovery, L-003549-00-0005), *HGS* (9146; Horizon Discovery, L-016835-00-0005) and non-targeting siRNAs (Horizon Discovery, D-001810-10-20) were purchased from Dharmacon. To generate stable knockdowns, cells were transduced with pLKO.1 lentiviral vectors expressing shRNAs targeting *RAB27A* (Sigma Aldrich, TRCN0000005295 [shRab27A¹]; Sigma Aldrich, TRCN0000005296 [shRab27A²]), and non-targeting shRNA (Sigma Aldrich, SHC002).

Retroviral and lentiviral packaging, infection, and selection

Retroviral pBABE expression vectors were packaged and target cells were transduced according to established protocols. Briefly, Phoenix-AMPHO cells (gift from C. McCormick, Dalhousie University) were seeded and transfected with retroviral vectors using polyethylenimine. Virus-containing CM was collected 2 d after transfection and clarified using a 0.45- μ M filter. Prior to infection, virus-containing medium was diluted 1:2 in DMEM growth medium and the mix was supplemented with Polybrene to a final concentration of 8 μ g ml⁻¹. Subsequently, the viral transduction mix (5 ml total volume/10 cm culture dish) was incubated with HEK293T cells for 24 h. Cells were selected 2 d post-transduction with 1 μ g ml⁻¹ puromycin for a minimum of 2 d. To package lentivirus, HEK293T cells were seeded and co-transfected with the packaging vectors pRSV-Rev, VSV.G, and pMDLg, and individual pLKO.1 transfer vectors. Virus collection, infection, and puromycin selection of stable cell pools were carried out as above.

EV preparation and characterization

EVs were purified according to standard differential centrifugation protocols⁶⁰. Briefly, cells seeded in 15-cm culture dishes at approximately 70% confluence were incubated with serum-free DMEM for 24 h. CM was collected and centrifuged serially at 200g for 5 min to pellet cells, 2,000g for 10 min to pellet cellular debris and apoptotic bodies, 10,000g for 30 min to pellet large EVs, and 100,000g in an ultracentrifuge for 3 h to pellet EVs. Crude EVs pellets were then gently triturated in PBS, diluted further in PBS (12 ml), and ultracentrifuged for an additional 70 min at 100,000g to generate EV preparations for further analysis as described below. Importantly, for all comparisons of EVs between experimental conditions, results from individual cohorts were

corrected as indicated on the basis of total cell number or WCL protein concentration to ensure that EV or EV protein quantification was not confounded by seeding differences.

Sucrose density gradient separation was utilized to generate highly purified EV preparations and to analyze the co-fractionation of TFRC, LC3-II, and EV marker proteins on linear sucrose gradients. Briefly, the 100,000g EV pellets generated via differential centrifugation as described above were thoroughly resuspended in 100 μ l 10% sucrose solution and gently layered onto a continuous 5–60% sucrose gradient formed on a gradient station (BioComp Instruments) and then ultracentrifuged at 210,000g for 18 h. Subsequently, 1 ml fractions from the gradient were top unloaded, weighed and diluted in 10 ml of PBS. The diluted fractions were spun at 100,000g for 70 min and the pellets were resuspended in RIPA lysis buffer for analysis by immunoblotting.

For protease protection assays, equal amounts of EVs were resuspended in PBS or PBS containing 1% Triton X-100 (EMD-Millipore, M1122980101) in the absence or presence of 100 μ g ml⁻¹ trypsin (Sigma Aldrich, T1426-100MG) for 30 min at 4 °C. Subsequently, the reactions were stopped by the addition of 2X protein sample buffer and the lysates were subjected to immunoblotting.

Antibodies

Immunoblotting: rabbit anti-M6PR (also known as IGF2R) (Abcam, ab124767; 1:5,000), mouse anti-LAMP2 (Santa Cruz Biotechnology, sc-18822; 1:200), mouse anti-CD71 (also known as TFRC) (Santa Cruz Biotechnology, sc-32272; 1:200), rabbit anti-LC3 (Cell Signaling Technology, 3868; 1:1,000), rabbit anti-CD63 (Abcam, ab134045; 1:1,000), mouse anti-TSG101 (BD Transduction Laboratories, 612696; 1:500), rabbit anti-CD71 (also known as TFRC) (Cell

Signaling Technology, 13113; 1:1,000), mouse anti-GAPDH (Millipore, MAB374; 1:5,000), rabbit anti-SQSTM1 (also known as p62) (Cell Signaling Technology, 39749; 1:1,000), rabbit anti-HA (Cell Signaling Technology, 3724; 1:5,000), mouse anti-myc (Millipore, M5546; 1:5,000), goat anti-firefly luciferase (Abcam, ab181640; 1:1,000), mouse anti-CD71 (also known as TFRC) (Santa Cruz Biotechnology, sc-65882; 1:200), rabbit anti-ATG7 (Cell Signaling Technology, 8558; 1:1,000), mouse anti-Alix (also known as PDCD6IP) (Cell Signaling Technology, 2171; 1:1,000), rabbit anti-HGS (Abcam, ab155539; 1:1,000), rabbit anti-RAB27A (Cell Signaling Technology, 69295; 1:1,000), peroxidase-AffiniPure donkey anti-rabbit IgG (H+L) (Jackson, 711-035-152; 1:5,000), peroxidase-AffiniPure donkey anti-mouse IgG (H+L) (Jackson, 715-035-150; 1:5,000), peroxidase-AffiniPure donkey anti-goat IgG (H+L) (Jackson, 705-035-147; 1:5,000).

For EV immuno-isolation: mouse anti-IgG2b kappa (eBioscience, 14-4732-82), mouse anti-CD63 (Abcam, ab8219), mouse anti-TFRC (Abcam, ab218326), mouse anti-TFRC (ProSci, 33-825), mouse anti-TFRC (NSJ Bioreagents, V3481).

Immunoblotting

To generate WCL and EV lysate, cells and EV preparations were lysed in RIPA buffer (Sigma Aldrich, R0278) (50 mM Tris, pH 8.0, 150 mM NaCl, 1% NP40, 0.5% sodium deoxycholate, 0.1% SDS) plus protease inhibitor cocktail (Sigma Aldrich, P8340) and PhosSTOP (Roche, 4906845001). Lysates were cleared by centrifugation, quantified by BCA assay (Thermo Fisher, 23225), mixed with sample buffer, resolved by SDS–polyacrylamide gel electrophoresis (PAGE) and transferred to polyvinylidene fluoride membrane. Membranes were blocked for 1 h in 5% milk in PBS with 0.1% Tween 20, incubated in primary antibody overnight at 4 °C, washed, incubated

for 1 h at room temperature with HRP-conjugated secondary antibodies (1:5,000; Jackson), washed and visualized via enhanced chemiluminescence (Millipore, WBLUF0100). Immunoblots were quantified by densitometry using Fiji and Image Lab.

Immunoprecipitation

For immunoprecipitation, cells transiently transfected with myc-tagged LC3 family members and TFRC-HA, TFRC(1-63)-Luc, or mutants thereof were lysed 24 h post-transfection in NP40 buffer (25 mM Tris, pH 8.0, 150 mM NaCl, 1% NP40, 5% glycerol, 2 mM EDTA, 2 mM EGTA, 10 mM β -glycerophosphate, 10 mM NaF) plus protease inhibitor cocktail (Sigma Aldrich, P8340) and PhosSTOP (Roche, 4906845001). Immune complexes were then captured by incubation with anti-c-myc magnetic beads (Thermo Scientific, 88842) for 2 h at 4 °C and then washed five times with NP40 buffer plus inhibitors, eluted with sample buffer and analyzed by immunoblotting.

Immuno-isolation of EVs

The following antibodies were employed for immuno-isolation of EVs: mouse anti-CD63 (Abcam, ab8219), mouse anti-TFRC (Abcam, ab218326; ProSci, 33-825; NSJ, V3481), and mouse IgG2b kappa isotype control (eBioscience, 14-4732-82). Briefly, 10 μ g of antibody against TFRC, CD63, or isotype control antibody was mixed with 50 μ L of Dynabeads Protein G (Invitrogen, 10003D) for 30 min and washed with PBS (0.1% BSA) to remove excess antibody. Subsequently, EVs purified from approximately 9×10^8 cells by differential centrifugation were resuspended in 100 μ L of PBS (0.1% BSA), split equally between four Eppendorf tubes (25 μ L each), and resuspended in 100 μ L PBS (0.1% BSA). Each sample was incubated with antibody-bound beads for 2 h at 4 °C with end-over-end rotation to allow capture of EVs. Next, bound EVs were captured

using the DynaMag-2 magnetic stand (Invitrogen, 12321D), washed 3x with ice-cold PBS (0.1% BSA) plus one final wash with PBS, and then eluted with 40 μ L of RIPA lysis buffer and sample buffer. Samples were then resolved via SDS-PAGE and immunoblotted for TFRC, LC3, and EV marker proteins.

Statistics and reproducibility

Statistical analyses were performed using Prism GraphPad 8 software. Groups were compared using unpaired Student's t-test where indicated or one-way ANOVA followed by Tukey's post-hoc test for multiple comparisons. The sample size was chosen on the basis of the size of the effect and variance for the different experimental approaches. P values of less than 0.05 were considered to be significant.

Chapter 3: Summary Discussion and Future Perspectives

Autophagy-Mediated Secretion of Transferrin Receptor in Extracellular Vesicles

Transferrin receptor was first identified in EVs during the 1980s. Since that discovery, TFRC+ EVs have been studied for their role in the shedding of unneeded proteins during reticulocyte maturation and their potential in therapeutic applications. However, the specific molecular components involved in the loading and secretion of TFRC in EVs has remained elusive. Previous studies have shown that, during reticulocyte maturation, the heat shock cognate 70 kDa protein (hsc70) interacts with the YTRF internalization motif of TFRC and may serve as a chaperone protein that promotes the sorting of TFRC into EVs. Additionally, co-immunoprecipitation assays demonstrated binding of the Alix homolog PalA to this region of TFRC, suggesting an additional interaction that may contribute to the EV sorting of TFRC⁶¹. Beyond these contributions, little is known about the molecular mechanisms involved in the loading and secretion of TFRC in EVs.

My studies highlight the role of autophagy in the secretion of TFRC in EVs. Specifically, I find that the LC3-conjugation machinery functionally contributes to the EV-mediated secretion of TFRC as a substrate of the LDELS pathway. Interestingly, disruption of components involved in LC3-conjugation ablates TFRC secretion while the disruption of pathway components required for classical degradative autophagy actually enhances TFRC secretion. This follows a recently emerging trend demonstrating that the disruption of degradative autophagy leads to an increase in secretory autophagy^{12,26}, perhaps as a means of compensation for the accumulated cellular waste. Additionally, I observe that TFRC binds ATG8 orthologs via a cytoplasmic domain LIR motif that coincides with the internalization motif of TFRC, which may facilitate the loading of TFRC into EVs. However, this LIR motif is not solely responsible for the functional secretion of TFRC. This may be explained by the observation that TFRC exists both in the conventionally annotated

orientation *and* in a reversed orientation in EVs, thus ATG8 proteins residing within the lumen of EVs may interact with LIRs localized to either the cytoplasmic *or* extracellular domains of TFRC. Alternatively, disruption of the cytoplasmic domain LIR may disrupt the normal homeostatic, autophagy-dependent secretion pathway and trigger an autophagy-independent mechanism to compensate for the loading and secretion of TFRC in EVs. Additionally, I observe that the secretion of TFRC requires specific ESCRT-associated components despite previously described LDELS substrates requiring nSMase2-dependent mechanism for secretion, suggestion that LDELS substrates may have substrate-specific mechanisms of intraluminal budding. Lastly, I observe that Rab27A, a small GTPase implicated in the docking of MVBs at the plasma membrane to release EVs, is functionally required for the secretion of TFRC, thus confirming that secreted TFRC comes from an endosomal origin (Supplemental Figure 3.1).

Overall, our results expand the protein cargo secreted via LDELS beyond our original description of RNA binding proteins by demonstrating that this secretory autophagy pathway mediates the incorporation of transmembrane proteins into EVs released outside of the cell. An important unanswered question is whether and how the LDELS modulates disease progression and physiological functions *in vivo*. In this regard, EVs containing TFRC have been connected to disease status and therapeutic applications in various contexts, including reticulocyte development, iron metabolism, and EV uptake³³⁻³⁵. Determining whether and how TFRC secretion via LDELS influences reticulocyte development and more broadly regulates cellular iron uptake and homeostasis remains an important topic for future study.

Reticulocyte Maturation

Erythrocytes, also known as red blood cells, are highly specialized cells dedicated to tissue oxygen delivery in mammals⁶². Erythrocytes develop from reticulocytes, which undergo extensive membrane remodeling and elimination of organelles during their maturation process⁶³. During erythropoiesis, autophagy plays a critical role in the clearance of organelles, including ribosomes and mitochondria, to allow proper development of mature red blood cells⁶⁴. Specifically, the loss of ATG7, a protein essential for LC3 lipidation and LC3 packaging into EVs, results in defective mitochondrial clearance^{13,65,66}. Furthermore, a hematologic lineage-specific knockout of *Atg7* *in vivo* resulted in severe anemia and an inability to selectively degrade mitochondria during erythropoiesis. Interestingly, these *Atg7*^{-/-} erythroid cells were shown to have increased levels of cell surface TFRC, suggesting an inability to properly shed this protein⁶⁶. Our data shows that the loss of ATG7 attenuates TFRC levels in EVs, suggesting that ATG7 plays a role in the shedding of TFRC via EVs. In further support, the timely clearance of mitochondria was recently demonstrated to be tightly coordinated with the shedding of TFRC during terminal reticulocyte maturation²⁶. In that sense, autophagy may contribute to the loading and secretion of TFRC in EVs that is required for the essential event of TFRC shedding during reticulocyte maturation.

The extensive role of autophagy in erythroid development highlights our need for a better understanding of the role that autophagy plays in the biogenesis and secretion of TFRC+ EVs. Patients with preleukemic disorders have been observed to have increased TFRC+ reticulocytes compared to healthy individuals³³, suggesting the improper shedding of TFRC is related to leukemia. Further research into the role of autophagy in TFRC+ EV secretion during reticulocyte maturation could confer novel insight into mechanisms underlying hematological disorders and possibly yield targets for novel therapeutics or evaluation of these disorders.

Iron Homeostasis

Transferrin receptor is known as the gatekeeper of iron metabolism as it is responsible for physiological iron acquisition by most cell types via the plasma glycoprotein transferrin⁶⁷. Transferrin comprises the most crucial ferric pool in the body as it transports iron through the blood to various tissues including the liver, spleen, and bone marrow⁶⁸. The expression of TFRCs is highly regulated by intracellular iron levels. Specifically, the absence of iron in the labile pool leads iron regulatory proteins (IRPs) to bind TFRC mRNA through iron response elements (IREs), thereby preventing mRNA degradation and increasing expression. Furthermore, research has shown that treatment with excess iron increases the ubiquitination and subsequent trafficking of TFRC to the multivesicular endosome (MVE)⁶⁹. Given that the MVE is the last stop for cargo before its release in EVs, it is plausible that treatment with excess iron also increases the secretion of TFRC in EVs.

Further supporting this notion, a recent study demonstrated that inducing oxidative stress in reticulocytes led to increased shedding of TFRC. The authors proposed this was a response of the cell to shed excess TFRC and ferric iron via EVs in order to reduce oxidative stress on the cell³³. Taken together, these studies support the notion that EV-mediated secretion of TFRC may serve as a means to mediate oxidative stress induced by excess iron in the cell. This is particularly interesting as TFRC levels are shown to positively correlate with ferroptotic cell death in cancer cells⁷⁰, thus understanding the mechanisms of TFRC shedding in response to oxidative stress could potentially inform responsiveness to cancer treatments. Further studies should investigate the role of the LC3-conjugation machinery in the proper shedding of TFRC within EVs in response to oxidative stress.

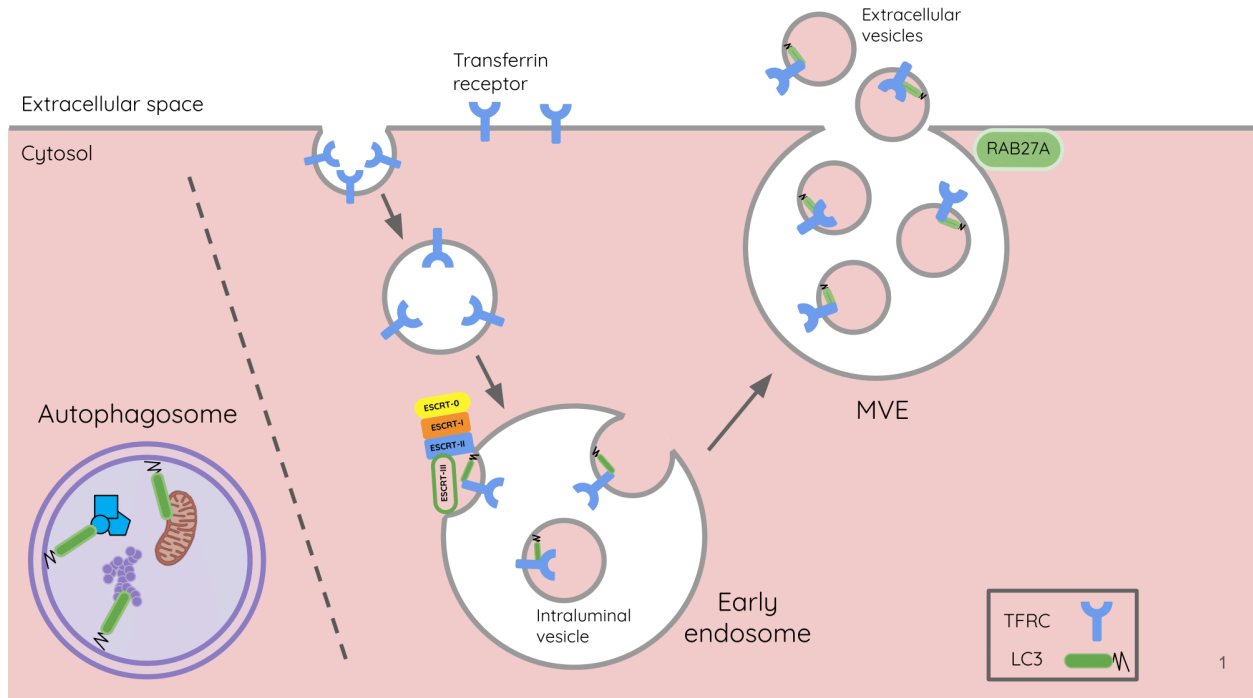
Extracellular Vesicle Uptake

EVs have generated growing interest for their ability to trigger phenotypic changes in acceptor cells. However, our knowledge of the uptake of EVs once they reach acceptor cells remains limited. There are three steps involved in EV uptake by an acceptor cell: targeting the acceptor cell, entry, and delivery of contents. The second step involves docking and internalization into the acceptor cell, which may involve a non-specific process, such as macropinocytosis, or a receptor-dependent pathway followed by clathrin-dependent endocytosis²³.

EV-associated TFRC may play an interesting role in this step of the EV uptake pipeline as evidenced by studies demonstrating a role for TFRC in EV docking. For example, employing TFRC antibodies to block accessibility of the receptor on the cell surface reduces the number of EVs uptaken by cells⁷¹, suggesting that TFRC may facilitate the uptake of EVs. This concept is further supported by another study in which pre-incubation of cells with transferrin, thereby enhancing TFRC internalization and reducing TFRC levels on the cell surface, reduces the uptake of EVs. Interestingly, pre-incubation of the EVs with transferrin enhances EV uptake, which led the authors to model a docking mechanism by which a dimer of transferrin binds transferrin receptors on the EVs and cell surface simultaneously thus docking the EV to the cell surface³⁵. Taken together, these data suggest TFRC may play a role in the successful entry of EVs into an acceptor cell. Given the involvement of the LC3-conjugation machinery in the secretion of EV-associated TFRC, future studies should investigate the contribution of this process to the docking and uptake of EVs.

Conclusion

This body of work highlights the role of autophagy in the secretion of transferrin receptor within extracellular vesicles. These studies identify transferrin receptor as a target of the LC3-dependent EV loading and secretion (LDELS) pathway. Overall, this work demonstrates the experimental foundation for assessing the molecular components involved in the selection, loading, and secretion of transmembrane proteins in extracellular vesicles.



Supplemental Figure 3.1: Proposed model for TFRC secretion in EVs via the LC3-dependent EV loading and secretion (LDELS) pathway.

TFRC is endocytosed at the plasma membrane and selected for secretion via the LC3-conjugation machinery in a process independent from classical degradative autophagy. Subsequently, the ESCRT pathway facilitates the intraluminal budding of TFRC into intraluminal vesicles thus forming a multivesicular endosome (MVE), which docks at the plasma membrane via the small GTPase RAB27A to release TFRC-containing EVs into the extracellular space.

References

1. Stolz A, Ernst A, Dikic I. Cargo recognition and trafficking in selective autophagy. *Nat Cell Biol.* 2014;16(6):495-501. doi:10.1038/ncb2979
2. Russell RC, Tian Y, Yuan H, et al. ULK1 induces autophagy by phosphorylating Beclin-1 and activating VPS34 lipid kinase. *Nat Cell Biol.* 2013;15(7):741-750. doi:10.1038/ncb2757
3. Ichimura Y, Kirisako T, Takao T, et al. A ubiquitin-like system mediates protein lipidation. *Nature.* 2000;408(6811):488-492. doi:10.1038/35044114
4. Johansen T, Lamark T. Selective autophagy mediated by autophagic adapter proteins. *Autophagy.* 2011;7(3):279-296. doi:10.4161/auto.7.3.14487
5. Birgisdottir ÅB, Lamark T, Johansen T. The LIR motif - crucial for selective autophagy. *J Cell Sci.* 2013;126(Pt 15):3237-3247. doi:10.1242/jcs.126128
6. Velikkakath AK, Nishimura T, Oita E, Ishihara N, Mizushima N. Mammalian Atg2 proteins are essential for autophagosome formation and important for regulation of size and distribution of lipid droplets. *Mol Biol Cell.* 2012;23(5):896-909. doi:10.1091/mbc.E11-09-0785
7. Jahn R, Scheller RH. SNAREs--engines for membrane fusion. *Nat Rev Mol Cell Biol.* 2006;7(9):631-643. doi:10.1038/nrm2002
8. Murrow L, Malhotra R, Debnath J. ATG12-ATG3 interacts with Alix to promote basal autophagic flux and late endosome function. *Nat Cell Biol.* 2015;17(3):300-310. doi:10.1038/ncb3112

9. Kaur J, Debnath J. Autophagy at the crossroads of catabolism and anabolism. *Nat Rev Mol Cell Biol.* 2015;16(8):461-472. doi:10.1038/nrm4024
10. Lock R, Kenific CM, Leidal AM, Salas E, Debnath J. Autophagy-dependent production of secreted factors facilitates oncogenic RAS-driven invasion. *Cancer Discov.* 2014;4(4):466-479. doi:10.1158/2159-8290.CD-13-0841
11. DeSelm CJ, Miller BC, Zou W, et al. Autophagy proteins regulate the secretory component of osteoclastic bone resorption. *Dev Cell.* 2011;21(5):966-974. doi:10.1016/j.devcel.2011.08.016
12. Solvik TA, Nguyen TA, Tony Lin YH, et al. Secretory autophagy maintains proteostasis upon lysosome inhibition. *J Cell Biol.* 2022;221(6):e202110151. doi:10.1083/jcb.202110151
13. Leidal AM, Huang HH, Marsh T, et al. The LC3-conjugation machinery specifies the loading of RNA-binding proteins into extracellular vesicles. *Nat Cell Biol.* 2020;22(2):187-199. doi:10.1038/s41556-019-0450-y
14. Guo H, Chitiprolu M, Roncevic L, et al. Atg5 Disassociates the V1V0-ATPase to Promote Exosome Production and Tumor Metastasis Independent of Canonical Macroautophagy. *Dev Cell.* 2017;43(6):716-730.e7. doi:10.1016/j.devcel.2017.11.018
15. Schorey JS, Cheng Y, Singh PP, Smith VL. Exosomes and other extracellular vesicles in host-pathogen interactions. *EMBO Rep.* 2015;16(1):24-43. doi:10.15252/embr.201439363
16. Deatherage BL, Cookson BT. Membrane vesicle release in bacteria, eukaryotes, and archaea: a conserved yet underappreciated aspect of microbial life. *Infect Immun.* 2012;80(6):1948-1957. doi:10.1128/IAI.06014-11

17. Robinson DG, Ding Y, Jiang L. Unconventional protein secretion in plants: a critical assessment. *Protoplasma*. 2016;253(1):31-43. doi:10.1007/s00709-015-0887-1
18. Johnstone RM, Adam M, Hammond JR, Orr L, Turbide C. Vesicle formation during reticulocyte maturation. Association of plasma membrane activities with released vesicles (exosomes). *J Biol Chem*. 1987;262(19):9412-9420.
19. van Niel G, D'Angelo G, Raposo G. Shedding light on the cell biology of extracellular vesicles. *Nat Rev Mol Cell Biol*. 2018;19(4):213-228. doi:10.1038/nrm.2017.125
20. Mallegol J, Van Niel G, Lebreton C, et al. T84-intestinal epithelial exosomes bear MHC class II/peptide complexes potentiating antigen presentation by dendritic cells. *Gastroenterology*. 2007;132(5):1866-1876. doi:10.1053/j.gastro.2007.02.043
21. Valadi H, Ekström K, Bossios A, Sjöstrand M, Lee JJ, Lötvall JO. Exosome-mediated transfer of mRNAs and microRNAs is a novel mechanism of genetic exchange between cells. *Nat Cell Biol*. 2007;9(6):654-659. doi:10.1038/ncb1596
22. Skotland T, Sandvig K, Llorente A. Lipids in exosomes: Current knowledge and the way forward. *Prog Lipid Res*. 2017;66:30-41. doi:10.1016/j.plipres.2017.03.001
23. Mathieu M, Martin-Jaular L, Lavieu G, Théry C. Specificities of secretion and uptake of exosomes and other extracellular vesicles for cell-to-cell communication. *Nat Cell Biol*. 2019;21(1):9-17. doi:10.1038/s41556-018-0250-9
24. Nolte-'t Hoen ENM, Buschow SI, Anderton SM, Stoorvogel W, Wauben MHM. Activated T cells recruit exosomes secreted by dendritic cells via LFA-1. *Blood*. 2009;113(9):1977-1981. doi:10.1182/blood-2008-08-174094

25. Chen G, Huang AC, Zhang W, et al. Exosomal PD-L1 contributes to immunosuppression and is associated with anti-PD-1 response. *Nature*. 2018;560(7718):382-386.
doi:10.1038/s41586-018-0392-8
26. Keller MD, Ching KL, Liang FX, et al. Decoy exosomes provide protection against bacterial toxins. *Nature*. 2020;579(7798):260-264. doi:10.1038/s41586-020-2066-6
27. Ponka P, Lok CN. The transferrin receptor: role in health and disease. *Int J Biochem Cell Biol*. 1999;31(10):1111-1137. doi:10.1016/s1357-2725(99)00070-9
28. Grosso R, Fader CM, Colombo MI. Autophagy: A necessary event during erythropoiesis. *Blood Rev*. 2017;31(5):300-305. doi:10.1016/j.blre.2017.04.001
29. Shen Y, Li X, Dong D, Zhang B, Xue Y, Shang P. Transferrin receptor 1 in cancer: a new sight for cancer therapy. *Am J Cancer Res*. 2018;8(6):916-931.
30. Feng H, Schorpp K, Jin J, et al. Transferrin Receptor Is a Specific Ferroptosis Marker. *Cell Rep*. 2020;30(10):3411-3423.e7. doi:10.1016/j.celrep.2020.02.049
31. Harding C, Heuser J, Stahl P. Endocytosis and intracellular processing of transferrin and colloidal gold-transferrin in rat reticulocytes: demonstration of a pathway for receptor shedding. *Eur J Cell Biol*. 1984;35(2):256-263.
32. Pan BT, Johnstone RM. Fate of the transferrin receptor during maturation of sheep reticulocytes in vitro: Selective externalization of the receptor. *Cell*. 1983;33(3):967-978.
doi:10.1016/0092-8674(83)90040-5
33. Zhang Q, Steensma DP, Yang J, Dong T, Wu MX. Uncoupling of CD71 shedding with mitochondrial clearance in reticulocytes in a subset of myelodysplastic syndromes.

Leukemia. 2019;33(1):217-229. doi:10.1038/s41375-018-0204-z

34. Yang L, Han D, Zhan Q, et al. Blood TfR⁺ exosomes separated by a pH-responsive method deliver chemotherapeutics for tumor therapy. *Theranostics*. 2019;9(25):7680-7696.
doi:10.7150/thno.37220
35. Qu M, Lin Q, Huang L, et al. Dopamine-loaded blood exosomes targeted to brain for better treatment of Parkinson's disease. *J Controlled Release*. 2018;287:156-166.
doi:10.1016/j.jconrel.2018.08.035
36. Johansen T, Lamark T. Selective Autophagy: ATG8 Family Proteins, LIR Motifs and Cargo Receptors. *J Mol Biol*. 2020;432(1):80-103. doi:10.1016/j.jmb.2019.07.016
37. New J, Thomas SM. Autophagy-dependent secretion: mechanism, factors secreted, and disease implications. *Autophagy*. 2019;15(10):1682-1693.
doi:10.1080/15548627.2019.1596479
38. Bel S, Pendse M, Wang Y, et al. Paneth cells secrete lysozyme via secretory autophagy during bacterial infection of the intestine. *Science*. 2017;357(6355):1047-1052.
doi:10.1126/science.aal4677
39. Durgan J, Lystad AH, Sloan K, et al. Non-canonical autophagy drives alternative ATG8 conjugation to phosphatidylserine. *Mol Cell*. 2021;81(9):2031-2040.e8.
doi:10.1016/j.molcel.2021.03.020
40. Heckmann BL, Teubner BJW, Tummers B, et al. LC3-associated endocytosis facilitates β -amyloid clearance and mitigates neurodegeneration in murine Alzheimer's Disease. *Cell*. 2019;178(3):536-551.e14. doi:10.1016/j.cell.2019.05.056

41. Olsvik HL, Svenning S, Abudu YP, et al. Endosomal microautophagy is an integrated part of the autophagic response to amino acid starvation. *Autophagy*. 2018;15(1):182-183.
doi:10.1080/15548627.2018.1532265
42. Sahu R, Kaushik S, Clement CC, et al. Microautophagy of cytosolic proteins by late endosomes. *Dev Cell*. 2011;20(1):131-139. doi:10.1016/j.devcel.2010.12.003
43. Mejlvang J, Olsvik H, Svenning S, et al. Starvation induces rapid degradation of selective autophagy receptors by endosomal microautophagy. *J Cell Biol*. 2018;217(10):3640-3655.
doi:10.1083/jcb.201711002
44. Lee C, Lamech L, Johns E, Overholtzer M. Selective Lysosome Membrane Turnover Is Induced by Nutrient Starvation. *Dev Cell*. 2020;55(3):289-297.e4.
doi:10.1016/j.devcel.2020.08.008
45. Hessvik NP, Llorente A. Current knowledge on exosome biogenesis and release. *Cell Mol Life Sci*. 2018;75(2):193-208. doi:10.1007/s00018-017-2595-9
46. Ostrowski M, Carmo NB, Krumeich S, et al. Rab27a and Rab27b control different steps of the exosome secretion pathway. *Nat Cell Biol*. 2010;12(1):19-30; sup pp 1-13.
doi:10.1038/ncb2000
47. Zhang H, Freitas D, Kim HS, et al. Identification of distinct nanoparticles and subsets of extracellular vesicles by asymmetric flow field-flow fractionation. *Nat Cell Biol*. 2018;20(3):332-343. doi:10.1038/s41556-018-0040-4
48. Harding CV, Heuser JE, Stahl PD. Exosomes: Looking back three decades and into the future. *J Cell Biol*. 2013;200(4):367-371. doi:10.1083/jcb.201212113

49. Clark DJ, Schnaubelt M, Hoti N, et al. Impact of Increased FUT8 Expression on the Extracellular Vesicle Proteome in Prostate Cancer Cells. *J Proteome Res.* 2020;19(6):2195-2205. doi:10.1021/acs.jproteome.9b00578
50. Ferreira JV, da Rosa Soares A, Ramalho J, et al. LAMP2A regulates the loading of proteins into exosomes. *Sci Adv.* 2022;8(12):eabm1140. doi:10.1126/sciadv.abm1140
51. Blanc L, De Gassart A, Géminard C, Bette-Bobillo P, Vidal M. Exosome release by reticulocytes—An integral part of the red blood cell differentiation system. *Blood Cells Mol Dis.* 2005;35(1):21-26. doi:10.1016/j.bcmd.2005.04.008
52. Jacomin AC, Samavedam S, Promponas V, Nezis IP. iLIR database: A web resource for LIR motif-containing proteins in eukaryotes. *Autophagy.* 2016;12(10):1945-1953. doi:10.1080/15548627.2016.1207016
53. Kumar M, Michael S, Alvarado-Valverde J, et al. The Eukaryotic Linear Motif resource: 2022 release. *Nucleic Acids Res.* 2021;50(D1):D497-D508. doi:10.1093/nar/gkab975
54. Green F, O'Hare T, Blackwell A, Enns CA. Association of human transferrin receptor with GABARAP. *FEBS Lett.* 2002;518(1-3):101-106. doi:10.1016/S0014-5793(02)02655-8
55. Cvjetkovic A, Jang SC, Konečná B, et al. Detailed Analysis of Protein Topology of Extracellular Vesicles—Evidence of Unconventional Membrane Protein Orientation. *Sci Rep.* 2016;6(1):36338. doi:10.1038/srep36338
56. Huotari J, Helenius A. Endosome maturation. *EMBO J.* 2011;30(17):3481-3500. doi:10.1038/emboj.2011.286
57. Trajkovic K, Hsu C, Chiantia S, et al. Ceramide triggers budding of exosome vesicles into

- multivesicular endosomes. *Science*. 2008;319(5867):1244-1247.
doi:10.1126/science.1153124
58. Desnos C, Schonn JS, Huet S, et al. Rab27A and its effector MyRIP link secretory granules to F-actin and control their motion towards release sites. *J Cell Biol*. 2003;163(3):559-570.
doi:10.1083/jcb.200302157
59. Leidal AM, Debnath J. Emerging roles for the autophagy machinery in extracellular vesicle biogenesis and secretion. *FASEB BioAdvances*. 2021;3(5):377-386. doi:10.1096/fba.2020-00138
60. Théry C, Amigorena S, Raposo G, Clayton A. Isolation and Characterization of Exosomes from Cell Culture Supernatants and Biological Fluids. *Curr Protoc Cell Biol*. 2006;30(1):3.22.1-3.22.29. doi:10.1002/0471143030.cb0322s30
61. Géminard C, de Gassart A, Blanc L, Vidal M. Degradation of AP2 During Reticulocyte Maturation Enhances Binding of Hsc70 and Alix to a Common Site on TfR for Sorting into Exosomes. *Traffic*. 2004;5(3):181-193. doi:10.1111/j.1600-0854.2004.0167.x
62. Jensen FB. The dual roles of red blood cells in tissue oxygen delivery: oxygen carriers and regulators of local blood flow. *J Exp Biol*. 2009;212(Pt 21):3387-3393.
doi:10.1242/jeb.023697
63. Ney PA. Normal and disordered reticulocyte maturation. *Curr Opin Hematol*. 2011;18(3):152-157. doi:10.1097/MOH.0b013e328345213e
64. Kundu M, Lindsten T, Yang CY, et al. Ulk1 plays a critical role in the autophagic clearance of mitochondria and ribosomes during reticulocyte maturation. *Blood*. 2008;112(4):1493-

1502. doi:10.1182/blood-2008-02-137398
65. Komatsu M, Waguri S, Ueno T, et al. Impairment of starvation-induced and constitutive autophagy in Atg7-deficient mice. *J Cell Biol.* 2005;169(3):425-434.
doi:10.1083/jcb.200412022
66. Mortensen M, Ferguson DJP, Edelmann M, et al. Loss of autophagy in erythroid cells leads to defective removal of mitochondria and severe anemia in vivo. *Proc Natl Acad Sci U S A.* 2010;107(2):832-837. doi:10.1073/pnas.0913170107
67. Richardson DR, Ponka P. The molecular mechanisms of the metabolism and transport of iron in normal and neoplastic cells. *Biochim Biophys Acta.* 1997;1331(1):1-40.
doi:10.1016/s0304-4157(96)00014-7
68. Ogun AS, Adeyinka A. Biochemistry, Transferrin. In: *StatPearls*. StatPearls Publishing; 2022. Accessed August 10, 2022. <http://www.ncbi.nlm.nih.gov/books/NBK532928/>
69. Tachiyama R, Ishikawa D, Matsumoto M, et al. Proteome of ubiquitin/MVB pathway: possible involvement of iron-induced ubiquitylation of transferrin receptor in lysosomal degradation. *Genes Cells.* 2011;16(4):448-466. doi:10.1111/j.1365-2443.2011.01499.x
70. Chen X, Yu C, Kang R, Tang D. Iron Metabolism in Ferroptosis. *Front Cell Dev Biol.* 2020;8. Accessed August 10, 2022. <https://www.frontiersin.org/articles/10.3389/fcell.2020.590226>
71. Gonda A, Kabagwira J, Senthil GN, et al. Exosomal survivin facilitates vesicle internalization. *Oncotarget.* 2018;9(79):34919-34934. doi:10.18632/oncotarget.26182

Publishing Agreement

It is the policy of the University to encourage open access and broad distribution of all theses, dissertations, and manuscripts. The Graduate Division will facilitate the distribution of UCSF theses, dissertations, and manuscripts to the UCSF Library for open access and distribution. UCSF will make such theses, dissertations, and manuscripts accessible to the public and will take reasonable steps to preserve these works in perpetuity.

I hereby grant the non-exclusive, perpetual right to The Regents of the University of California to reproduce, publicly display, distribute, preserve, and publish copies of my thesis, dissertation, or manuscript in any form or media, now existing or later derived, including access online for teaching, research, and public service purposes.

DocuSigned by:

Jackson Gardner

7FE299BB40CE47F...

Author Signature

12/13/2022

Date